Chemical Science

ROYAL SOCIETY OF CHEMISTRY

EDGE ARTICLE

View Article Online
View Journal | View Issue

Open Access Article. Published on 03 March 2022. Downloaded on 10/28/2025 3:34:55 PM.
This article is licensed under a Creative Commons Attribution-NonCommercial 3.0 Unported Licence.

Check for updates

Cite this: *Chem. Sci.*, 2022, **13**, 3775

All publication charges for this article have been paid for by the Royal Society of Chemistry

Synthesis of distibiranes and azadistibiranes by cycloaddition reactions of distibenes with diazomethanes and azides†

Hanns M. Weinert,[a] Christoph Wölper[a] and Stephan Schulz *[ab]

Cycloaddition reactions of distibene $[L(Me_2N)GaSb]_2$ (L = HC[C(Me)NDipp]$_2$; Dipp = 2,6-*i*-$Pr_2C_6H_3$)= with a series of organoazides RN_3 (R = Ph, *p*-CF_3Ph, 1-adamantyl (ada)) yielded azadistibiranes $[L(Me_2N)GaSb]_2NR$ (R = Ph **1**, *p*-CF_3Ph **2**, ada **3**), whereas Me_3SiN_3 reacted with insertion into one Ga–Sb bond and formation of $L(Me_2N)GaSbSb(NSiMe_3)Ga(NMe_2)L$ (**4**). Analogous compounds **5** and **6** formed after heating of **1** and **2** above 60 °C. Prolonged heating of **5** resulted in a [2 + 2] cycloaddition accompanied by elimination of $LGa(NMe_2)_2$ and formation of tetrastibacyclobutane **7**, while the reaction of **5** with a second equivalent of PhN_3 gave heteroleptic azadistibirane **9**, which isomerized at elevated temperature to distibene **10**. Cycloaddition also occurred in reactions of $[L(X)GaSb]_2$ (X = NMe_2, OEt, Cl) with $Me_3Si(H)CN_2$, yielding distibiranes $[L(X)GaSb]_2C(H)SiMe_3$ (X = NMe_2 **11**, OEt **12**, Cl **13**). Compounds **1–13** were characterized by IR, UV-Vis and NMR spectroscopy and sc-XRD. The mechanism of the reaction of $[L(Me_2N)GaSb]_2$ with PhN_3 and Me_3SiN_3 and the electronic nature of the resulting compounds were studied by DFT calculations.

Received 18th January 2022
Accepted 3rd March 2022

DOI: 10.1039/d2sc00314g

rsc.li/chemical-science

Introduction

Homonuclear main group element compounds with π bonding contribution have received increasing interest in the last decade due to their promising reactivity in small molecule activation reactions including catalytic processes.[1] Double-bonded species in principle should undergo cycloaddition reactions, which belong to the most versatile synthetic tools in organic chemistry (*i.e.* Diels–Alder reaction and Huisgen cycloaddition).[2] Heavier homologues of alkenes, disilenes R_2SiSiR_2 and digermenes R_2GeGeR_2,[3] as well as diphosphenes RPPR were successfully applied in a variety of [2 + *n*] (*n* = 1–4) cycloaddition reactions,[4] and diphosphenes reacted with formation of diphosphiranes and azadiphosphiranes (Scheme 1), respectively. In remarkable contrast, virtually no reactions of heavier group 15 dipnictenes RPnPnR containing Pn–Pn double bonds (Pn = As, Sb, Bi) are known, most likely originating from the use of sterically demanding organic substituents, which are applied to avoid the thermodynamically favored dimerization of heavier dipnictenes to cyclotetrapnictanes (kinetic stabilization), which were obtained from reduction reactions of $RPnX_2$ (X = halide).[5] Their formation can be rationalized by [2 + 2] cycloaddition of transient dipnictenes, however, the reaction of isolated dipnictene to cyclotetrapnictanes was not yet reported. Diels–Alder-type cycloaddition reactions were only reported for trapped (transient) diarsenes containing sterically less demanding

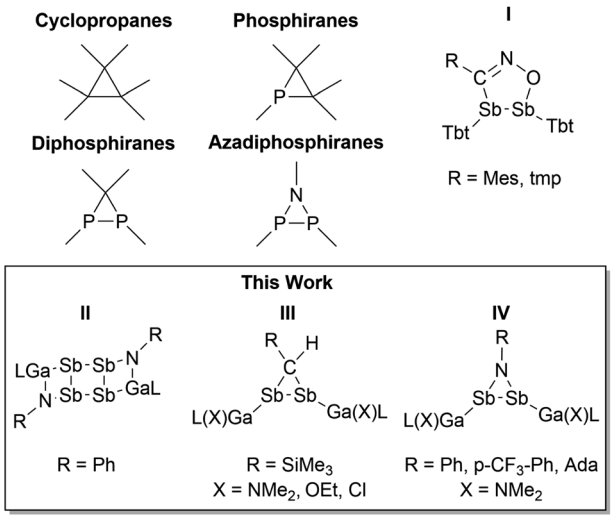

Scheme 1 Heterocycles formed in cycloaddition reactions of dipnictenes.

[a]*Institute for Inorganic Chemistry, University of Duisburg-Essen, Universitätsstraße 5–7, 45117 Essen, Germany. E-mail: stephan.schulz@uni-due.de*

[b]*Center for Nanointegration Duisburg-Essen (Cenide), University of Duisburg-Essen, Carl-Benz-Straße 199, 47057 Duisburg, Germany*

† Electronic supplementary information (ESI) available: Detailed synthetic procedures and analytical data, NMR, IR, and UV-Vis spectra of **1–13**, computational details and cif files. CCDC 2129215 (**1**), 2129216 (**2**), 2129217 (**3**), 2129218 (**4**), 2129219, (**5**), 2129220, (**6**), 2129221 (**7**), 2129222 (**8**), 2129223 (**9**), 2129211 (**10**), 2129212 (**11**), 2129213 (**12**), and 2129214 (**13**). For ESI and crystallographic data in CIF or other electronic format see DOI: 10.1039/d2sc00314g

© 2022 The Author(s). Published by the Royal Society of Chemistry

Open Access Article. Published on 03 March 2022. Downloaded on 10/28/2025 3:34:55 PM.
This article is licensed under a Creative Commons Attribution-NonCommercial 3.0 Unported Licence.

substituents,[6] *e.g.* 2,3-bistrifluoromethyl-2,3-arsabicyclo[2.2.2]oct-5-ene was formed in a trapping reaction of *in situ* formed $[CF_3As]_2$ with cyclohexadiene.[6a] The 1,3 dipolar cycloaddition of nitrile oxides (tmp)CNO (tmp = 2,4,6-$(MeO)_3C_6H_2$, 2,4,6-$Me_3C_6H_2$) reported by Ohashi *et al.* to the best of our knowledge therefore represents the only cycloaddition reaction of a distibene (**I**).[7] This group also reported on the formation of a single product in the reaction of $[(Bbt)Sb]_2$ (Bbt = 2,6-$[CH(SiMe_3)_2]$-4-$[C(SiMe_3)_3]$-C_6H_2) with Me_3SiN_3, but the as-formed compound could not be isolated due to its thermal instability. Apart from these studies, only reactions of distibenes with chalcogens were reported,[5e,f,7a,8] yielding three-membered seleno- and tellurodistibirane rings.

We are generally interested in the reactivity of electron-rich L(X)Ga-substituted dipnictenes of the type $[L(X)GaE]_2$ (E = As, Sb, Bi),[9] and recently reported on cyclic voltammetry (CV) studies and single electron reduction reactions, yielding distibene and dibismuthene radical anions.[10] We now extended our studies to cycloaddition reactions and herein report on reactions of distibenes $[L(X)GaSb]_2$ (X = Cl, OEt, NMe_2) with diazomethane $Me_3Si(H)CN_2$ and a series of organoazides RN_3, yielding distibiranes (**III**) and azadistibiranes (**IV**), which were found to rearrange upon heating with re-formation of the Sb–Sb double bond and finally to tetrastibacyclobutane (**II**).

Results and discussion

Synthesis

$[L(Me_2N)GaSb]_2$ [9a] unselectively reacted with organoazides RN_3 at ambient temperature with N_2 elimination and formation of several reaction products according to ^{1}H NMR spectroscopic studies (Fig. S46†). In contrast, dropwise addition of toluene solutions of PhN_3, *p*-CF_3PhN_3 and 1-adaN_3 to a cooled (−30 °C) suspension of $[L(Me_2N)GaSb]_2$ and slow heating to ambient temperature selectively gave azadistibiranes **1–3** (Scheme 2). The reactions can be classified in a formal sense as [2 + 1] cycloaddition reactions, but an initial [2 + 3] dipolar cycloaddition followed by a rapid N_2 elimination is also plausible.[2,4a,11] However, temperature-dependent *in situ* ^{1}H NMR spectroscopic studies, which were hampered by the low solubility of $[L(Me_2N)GaSb]_2$, did not show any additional (intermediate) resonances others than those of azadistibirane **1**, hence providing no hints for a [2 + 3] cycloaddition mechanism (Fig. S47†). In contrast, the analogous reaction with Me_3SiN_3 occurred with insertion of the nitrene into the Ga–Sb bond and subsequent formation of $L(Me_2N)GaSbSb(NSiMe_3)Ga(NMe_2)L$ (**4**). Comparable findings were reported by Weigand *et al.* for reactions of diphosphenes with RN_3, yielding azadiphosphiranes with aryl azides but imine-substituted diphosphene with Me_3SiN_3.[12]

The yield of azadistibiranes **1–3** significantly dropped with increasing reaction times. At ambient temperature, toluene solutions of **1** and **2** underwent slow rearrangement of the nitrene unit and formation of compounds **5** and **6**, while heating above 80 °C greatly increases the reaction speed. Azadistibirane **3** in contrast is thermally more stable and was found to decompose unselectively starting at 80 °C. We failed to isolate compound **5** and **6** in pure form due to their slow decomposition in solution (see ^{1}H-NMR Fig. S15 and S18†). Prolonged heating of **5** at 100 °C for 120 h resulted in complete decomposition with formation of $LGa(NMe_2)_2$ and tetrastibacyclobutane $[(L(NPh)Ga\text{-}\kappa Ga,\kappa N)_2\text{-}(\mu,\eta^{1:1:1:1}\text{-}Sb_4)]$ **7**, which precipitated due to its low solubility in toluene.

$[L(Me_2N)GaSb]_2$ was also reacted with two equivalents of Me_3SiN_3, yielding a mixture of two species. Only the major species **8**, in which in contrast to compound **4** one NMe_2 group is additionally replaced by an amide group ($N(H)SiMe_3$), was isolated by precipitation upon slow diffusion of CH_3CN into the toluene solution. The formation of **8** is unclear, and both toluene and the methyl group of the β-diketiminate ligand can serve as the proton source.[13] In contrast, compound **5** was found to react cleanly with a second equivalent of PhN_3 to azadistibirane **9**, which isomerized to distibene **10** upon heating to 70 °C as well.

We also reacted distibenes $[L(X)GaSb]_2$ (X = NMe_2, OEt, Cl) with $Me_3Si(H)CN_2$ at ambient temperature (Scheme 3), yielding distibiranes $[L(X)GaSb]_2C(H)SiMe_3$ (X = NMe_2 **11**, OEt **12**, Cl **13**)

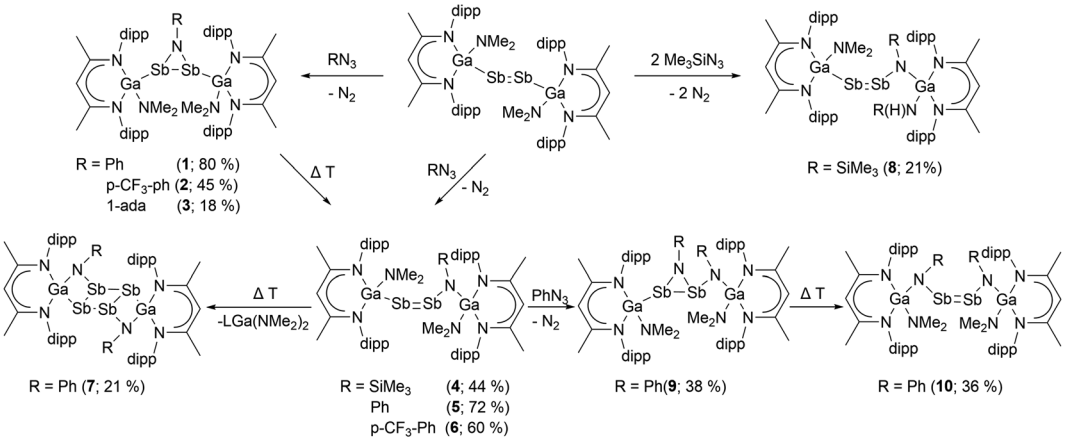

Scheme 2 Azadistibiranes **1–3** and distibenes **4–6** formed by cycloaddition reactions of distibene $[L(Me_2N)GaSb]_2$ with organoazides. **5** dimerizes to cyclotetrastibane **7** upon thermal treatment and reacts with a second equivalent of PhN_3 to **9**, which isomerizes to **10** upon heating.

 © 2022 The Author(s). Published by the Royal Society of Chemistry

Open Access Article. Published on 03 March 2022. Downloaded on 10/28/2025 3:34:55 PM.
This article is licensed under a Creative Commons Attribution-NonCommercial 3.0 Unported Licence.

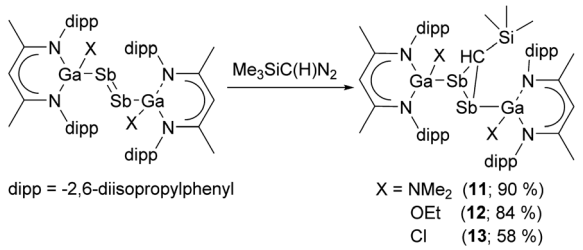

Scheme 3 Cycloaddition reactions of $[L(X)Ga]_2$ with $Me_3Si(H)CN_2$ to distibiranes **11–13**.

with high selectivity. A low temperature *in situ* ^{1}H NMR study showed that the reaction of $[L(Me_2N)GaSb]_2$ is fast and even at −80 °C no reaction intermediates were detected (Fig. S48†). Distibiranes **11–13** did not react with additional equivalents of diazomethane or azides even at elevated temperature (100 °C).

Spectroscopic characterization

All compounds except **7** and **10** are soluble in non-polar solvents such as *n*-hexane and toluene or solvents of intermediary polarity such as thf, while they are insoluble in polar solvents, *i.e.*, DMF or acetonitrile. **7** and **10** are only slightly soluble in toluene or benzene. They exhibit the typical resonance for the L(X)Ga ligand with characteristic singlets around 5 ppm (γ-H) and 1.5–2 ppm (Me) of the β-diketiminate ligand, as well as sets of doublets (2–0.5 ppm) and septets (4.5–2.5 ppm) for the isopropyl groups. Azadistibiranes **1** and **2** each exhibit a set of resonance for the *ortho*-protons of the phenyl group, which are shifted to 5.28 and 5.1 ppm, respectively. This shift to higher field is less pronounced for **9** (5.9–6.1 ppm) and likely caused due to the proximity to the Dipp groups, while insertion products **5**, **6**, and **10** and tetrastibacyclobutane **7** exhibit this resonance in the typical range of aromatic amines. The proton resonances of the Me_3SiN units in **4** and **8** are found at 0.4 and 0.5 ppm and the N(*H*)$SiMe_3$ resonances in **8** at −0.6 ppm. Distibiranes **11–13** are unsymmetric molecules (C1 symmetry) with restricted rotation, hence all carbon atoms (except Me_3Si) are magnetically inequivalent, leading to two γ-H, four Me singlets, 16 doublets and 8 septets for the Dipp ligands, while the C*H*$SiMe_3$ resonances are found at 1.81, 2.13 and 2.18 ppm, respectively. In contrast, azadistibiranes **1–3** each show only a single resonance for both γ-H atoms. This finding either points to trigonal planar-coordinated N atoms (compare R–C/N–*Δ* angle Table 2), to fast inversion processes or to an equilibrium between the azadistibirane and the distibaimine **15** (see Scheme 4). Since our calculated thermodynamic energies (Scheme 4) don't support the formation of such an equilibrium, we explain these findings by fast inversion processes, since the inversion of ternary amines, in contrast to the heavier pnictogens, is typically very fast at room temperature.[14]

UV-Vis spectra of toluene solutions of **4–6** and **8** show adsorption bands for the π → π* transition between 494 and 502 nm,[15] while **10** shows an absorption maxima at 584 nm (Fig. S50†), which is red shifted compared to $[L(Me_2N)GaSb]_2$ (430 nm)[10] and to amido-substituted distibenes (510–514 nm).[16]

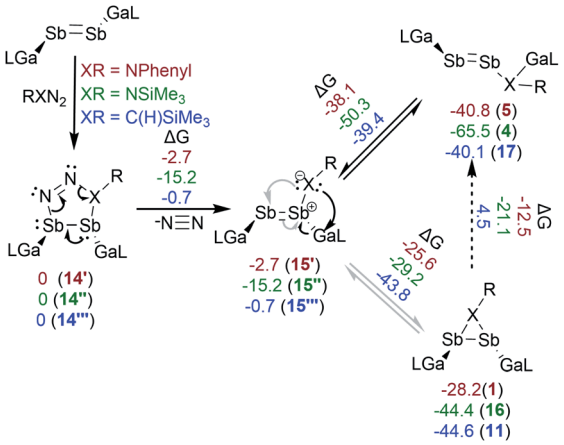

Scheme 4 Proposed reaction mechanism for the azadistibiranes and amidodistibenes formation from reactions with PhN_3 and Me_3SiN_3. Free Gibbs energies (normalized to the respective 1,2-distibatriazene in kcal mol^{-1}) of the optimized structures at the PBE0/def2-SVP(D3BJ) level of theory are given.

The red shift indicates a smaller π–π* energy gap, most likely due to the π-donating NMe_2 groups, which increase the energy level of the π-orbitals relative to the π*-orbitals and hence decrease the transition energy (Fig. 2).[17] In contrast, toluene solutions of azadistibiranes **1–3** and distibiranes **11–13** are slightly orange and yellow and only show weak adsorption bands at the edge of the visible spectrum (Fig. S49 and S52†), which are partially overlayed by the adsorption of the L(Me_2N)Ga ligand.[10b]

Single crystal X-ray structures

The molecular structures of **1–13** were determined by sc-XRD. Single crystals were obtained from solutions in *n*-pentane (**13**, Fig. S58†), *n*-hexane (**4**, Fig. S55;† **6**, Fig. S56†), benzene (**11**, Fig. S57†) and toluene (**1**, **7**, **9**, **10**, Fig. 1; **2**, Fig. S53†) upon storage at ambient temperature (**7**, **9**, **10**), 7 °C (**11**) or −30 °C (**1**, **2**, **4**, **13**) for 48 h, respectively. Single crystals of **12** (Fig. 1) were formed upon slow evaporation of a *n*-hexane solution and those of **3** (Fig. S54†), **5** (Fig. 1) and **8** (Fig. 1) by slow diffusion of CH_3CN into toluene solutions. **2** and **9–11** crystallize in the triclinic crystal system (Tables S1a and b†) and all others in the monoclinic crystal system. Selected bond lengths and angles of distibenes **4–6**, **8** and **10** are summarized and compared to those of $[L(Me_2N)GaSb]_2$ in Table 1. The Sb–Sb bonds in the distibenes (2.6541(4) **4**; 2.6750(3) **5**; 2.6627(3) **6**; 2.6534(5) **8**; 2.6688(1) Å **10**) are slightly elongated compared to that of $[L(Me_2N)GaSb]_2$ (2.6477(3) Å). Remarkably, distibenes **4–6** show short intramolecular N···Sb distances (2.472(3) **4**; 2.395(1) **5**; 2.424(2) Å **6**) between the NMe_2 group and the neighboring Sb atom and elongated (by 0.1 Å) Ga–NMe_2 bonds. This was neither observed for distibene $[L(X)GaSb]_2$ nor **8** and **10**. Distibenes **4–6** also exhibit shorter Ga–Sb bond lengths (2.5836(5) **4**; 2.5842(3) **5**; 2.5834(4) Å **6**) compared to that of $[L(Me_2N)GaSb]_2$ (2.6200(4) Å). The electronegative imine ligand most likely increases the

Open Access Article. Published on 03 March 2022. Downloaded on 10/28/2025 3:34:55 PM.
This article is licensed under a Creative Commons Attribution-NonCommercial 3.0 Unported Licence.

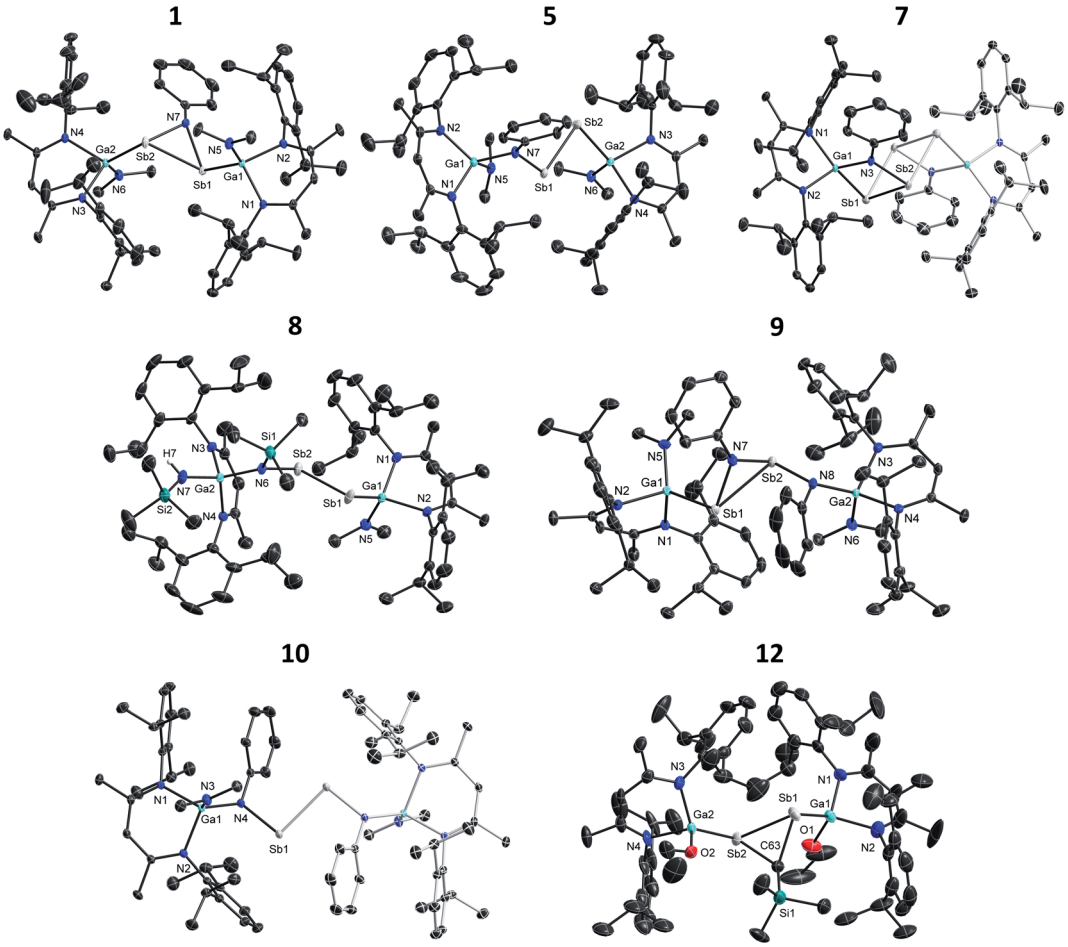

Fig. 1 Molecular structures of $[L(Me_2N)GaSb]_2NPh$ (**1**), $[L(Me_2N)Ga]SbSb[N(Ph)Ga(NMe_2)L]$ (**5**), $[(L(PhN)Ga\text{-}\kappa Ga,\kappa N)_2\text{-}(\mu,\eta^{1:1:1:1}\text{-}Sb_4)]$ (**7**), $[L(Me_2N)Ga]SbSb[N(SiMe_3)Ga(N(H)SiMe_3)L]$ (**8**), $[L(Me_2N)GaSb][L(Me_2N)GaN(Ph)Sb]NPh$ (**9**), $[L(Me_2N)GaN(Ph)Sb]_2$ (**10**), and $[L(EtO)GaSb]_2C(H)SiMe_3$ (**12**). H atoms are omitted for clarity and displacement ellipsoids are drawn at the 50% probability level. For **7** and **10** the symmetry generated part is displayed in pale colors.

electrophilicity of the Sb atom, which favors a dative intramolecular interaction of the amine group.

Selected bond lengths and angles of azadistibiranes **1–3**, and **9** and distibiranes **11–13** are summarized in Table 2. Generally, the Sb–Sb bond is significantly elongated compared to $[L(Me_2N)GaSb]_2$ (2.6477(3) Å) ranging from 2.7882(2) Å (**1**) to 2.8291(3) Å (**9**) and thus lying in the typical range observed for distibanes Sb_2R_4 (2.77–3.07 Å).[18] The Sb–C/N bonds (Sb–C: 2.14–2.29 Å; Sb–N: 2.08–2.11 Å) are in the typical single bond range (Sb–C: 2.04–2.31 Å; Sb–N: 1.95–2.58 Å)[19] and the Sb–N–Sb bond angles of the azadistibiranes (83.15(4) **1**; 83.0(1) **2**; 83.3(1) **3**; 87.28(7)° **9**) are slightly larger than those of the distibiranes (78.0(1) **11**; 78.4(2)

Table 1 Selected bond lengths [Å] and angles [°] of distibenes **4–6**, **8**, **10** and of the parent distibene $[L(Me_2N)GaSb]_2$ [9a] for comparison

	$[L(Me_2N)GaSb]_2$[c]	**4**	**5**	**6**	**8**	**10**[c]
Sb–Sb	2.6477(3)	2.6541(4)	2.6750(3)	2.6627(3)	2.6534(5)	2.6688(1)
Sb–Ga	2.6200(4)	2.5836(5)	2.5842(3)	2.5834(4)	2.6241(5)	3.2907(4)
Sb–N	—	2.089(2)	2.096(1)	2.111(2)	2.071(2)	2.0727(8)
Sb–(NMe_2)	3.825(1)	2.472(3)	2.395(1)	2.424(2)	5.102(3)[b]	3.865(1)
Ga–N	—	1.863(2)	1.865(1)	1.874(2)	1.917(2)	1.8818(8)
Ga–(NMe_2)[a]	1.856(1)	1.943(2)	1.955(1)	1.949(2)	1.857(2)[b]	1.8524(8)
N–Sb–N[a]	—	74.71(9)	72.54(5)	72.53(8)	—	—
N–Ga–N[a]	—	94.0(1)	88.57(5)	89.60(9)	—	—
|N–Sb–Ga–N|[a]	—	171.2(1)	152.52(8)	166.0(2)	—	—

[a] Values are discussed for the amido substituted part. [b] Here $N(H)SiMe_3$. [c] Inversion symmetry.

 © 2022 The Author(s). Published by the Royal Society of Chemistry

Open Access Article. Published on 03 March 2022. Downloaded on 10/28/2025 3:34:55 PM. This article is licensed under a Creative Commons Attribution-NonCommercial 3.0 Unported Licence.

Table 2 Selected bond lengths [Å] and angles [°] of azadistibiranes **1**–**3** and **9**, and distibiranes **11**–**13**[a]

	Sb–Sb	Sb–C/N	Sb–Ga	Sb–C/N–Sb	C/N–Sb–Sb	Ga–Sb–Δ	R–C/N–Δ
1	2.7882(2)	2.114(1)	2.6520(2)	83.15(4)	48.84(3)	102.90(2)	140.2(1)
		2.087(1)	2.6564(2)		48.01(3)	104.91(3)	
2	2.778(3)[b]	2.113(3)	2.6434(3)	83.0(1)[b]	48.98(9)[b]	101.82(2)[b]	141.9(5)[b]
		2.080(3)[b]	2.649(3)[b]		48.00(9)[b]	103.7(1)[b]	
3	2.7987(4)	2.099(3)	2.6477(4)	83.3(1)	48.56(8)	104.67(2)	143.4(3)
		2.113(3)	2.6950(5)		48.13(8)	110.71(3)	
9	2.8291(3)	2.080(2)	2.6540(3)	87.28(7)	45.48(5)	102.36(2)	171.9(2)
		2.019(2)	2.058(2)[d]		47.24(5)	101.03(5)[d]	
11	2.7912(5)	2.139(3)[c]	2.6431(6)	78.0(1)[c]	48.55(9)[c]	114.56(3)[c]	138.4(3)[c]
		2.294(4)[c]	2.6400(6)		53.48(9)[c]	100.25(3)[c]	
12	2.7912(7)	2.219(8)	2.623(1)	78.4(2)	51.2(2)	93.67(6)	142.3(6)
		2.196(8)	2.627(1)		50.4(2)	105.94(5)	
13	2.7991(3)	2.225(4)[c]	2.6213(4)	79.2(1)[c]	51.3(1)[c]	96.70(3)[c]	135.9(3)[c]
		2.164(4)[c]	2.6521(4)		49.4(1)[c]	107.34(2)[c]	

[a] Δ: centre of the plane span by Sb–Sb–C/N triangle. [b] Values are discussed for average of the disordered L(Me_2N)GaSbN-p-CF_3–Ph part. [c] Values are discussed for the major component of the disordered C(H)$SiMe_3$ part. In both cases the values should be interpreted with caution. [d] N(Ph) instead of Ga.

12; 79.2(1)° **13**). The angles deviate from the ideal tetrahedral angle for a sp^3-hybridized N atom and from the 90° angle expected for an unhybridized Sb atom, most likely resulting from the ring strain. Although the azadistibiranes have formally six electrons (three pnictogen electron lonepairs), Hückel aromaticity can be excluded since both Sb ligands adopt almost perpendicular orientations to the plane in the *E* configuration (94–115°; Table 2) and the bond length within the three-membered rings are more in line with single bonds.

Tetrastibacyclobutane **7** shows an inversion center in the Sb_4 plane. The Sb–Sb bond lengths (2.8837(2), 2.8449(2) Å) and Sb–Sb–Sb bond angles (94.982(6), 85.018(6)°) within the Sb_4 ring slightly deviate from those expected for an ideal square. The Ga–N (1.890(2) Å), Sb–N (2.083(2) Å) and Ga–Sb bond lengths (2.6221(3) Å) are in the typical range of single bonds. The almost flat Ga–Sb–Sb–N unit (torsion angle of −4.13(5)°) resembles a distorted trapezoid, which adopts a perpendicular orientation to the Sb_4 plane. The Sb–Sb bond lengths are in the typical range reported for Sb–Sb single bonds,[18] whereas the shortest diagonal Sb–Sb distance (4.2230(4) Å) is far longer than that observed in [{L(X)Ga}$_2$-μ,η$^{1:1}$-Sb_4] obtained directly from thermolysis of [L(Me_2N)GaSb]$_2$.[9a,b]

Quantum chemical calculations

The reactions of [L(Me_2N)GaSb]$_2$ with PhN_3 and Me_3SiN_3 were investigated by quantum chemical calculations at the PBE0 level of theory.[20] Weigand *et al.* proposed for reactions of the diphosphene cation [($^{Cl}Im^{Dipp}$)P=P(Dipp)]$^+$ with RN_3 (R = Me_3Si, Dipp) the initial formation of diphosphatriazoles *via* 1,3-dipolar cycloaddition,[12] which upon elimination of N_2 either formed diphospheneimine (Me_3SiN_3) or rearranged to azadiphosphirane ($DippN_3$). A similar mechanism is likely in our reactions with PhN_3 and Me_3SiN_3, and both the distibatriazole (**14**) and the distibaimine (**15**) were found as minima on the energy surface (Scheme 4). The elimination of N_2 by a retro [3 + 2] cycloaddition reaction is energetically favored by −15 (Me_3SiN_3) and −3 kcal mol^{-1} (PhN_3), respectively, which is more than 14 kcal mol^{-1} less favored compared to the phosphorous species. This might explain why Tokitoh *et al.* observed no reactivity of [(Bbt)Bi]$_2$ in cycloaddition reaction compared to [(Bbt)Sb]$_2$.[7b] The formation of both imine structures is thermodynamically unfavored and were not observed by ^{1}H NMR spectroscopy, but they are still likely intermediates in the rearrangement of azadistibiranes to distibenes **4** and **5**. The ΔG values of 25–30 kcal mol^{-1} are in line with slow transformations at 20 °C but fast at 100 °C, but different pathways for the rearrangement reactions can't be excluded.

In case of $NSiMe_3$-substituted species, compound **4** is almost 9 kcal mol^{-1} more favored than compound **5** with respect to the corresponding azadistibiranes **16** and **1**, although this finding is not directly related to the activation barrier. The experimental findings suggest that for **15''** the [1,2] sigmatropic shift reaction to **4** is both kinetically and thermodynamically favored, whereas compound **1** was isolated in almost quantitative yield upon performing the reaction at low temperature.

A similar mechanism was postulated for reactions of diphosphenes with diazomethanes, and the (intermediary) formation of hydro-diphosphapyrazol and methylene-diphosphene was observed by *in situ* ^{31}P-NMR spectroscopy.[21] We identified the corresponding hydrodistibapyrazol (**14'''**), methylenedistibene (**15'''**) and the insertion product (**17**) as minima on the energy surface (Scheme 4). In contrast to the azadistibiranes (**1**, **16**), the corresponding distibirane **11** is energetically favored by 4.5 kcal mol^{-1} compared to the respective insertion product **17**, explaining the higher thermal stability of **11**. In addition, the energy difference between **15'''** and **11** (43.8 kcal mol^{-1}) is much larger than those observed for the corresponding imine compounds **15'** *vs.* **1** (25.6 kcal mol^{-1}) and **15''** *vs.* **16** (29.2 kcal mol^{-1}), respectively, making its formation upon heating rather unlikely. This perfectly agrees with our experimental findings since no intermediates were observed even at very low reaction temperatures (−80 °C).

Open Access Article. Published on 03 March 2022. Downloaded on 10/28/2025 3:34:55 PM.
This article is licensed under a Creative Commons Attribution-NonCommercial 3.0 Unported Licence.

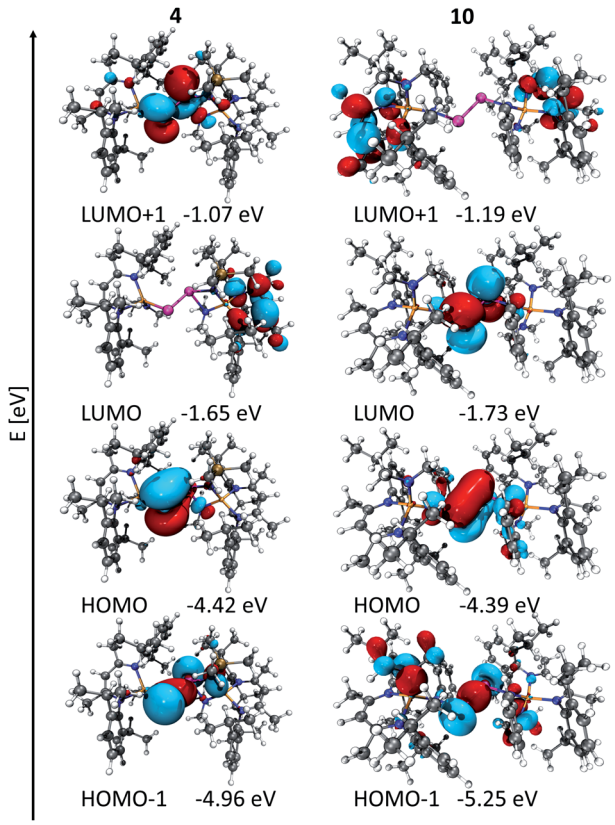

Fig. 2 Section of the MO diagram of [L(Me_2N)GaSbSbN($SiMe_3$)Ga(NMe_2)L] (**4**) and [L(Me_2N)Ga(NPh)Sb]$_2$ (**10**), isovalue 0.03.[23]

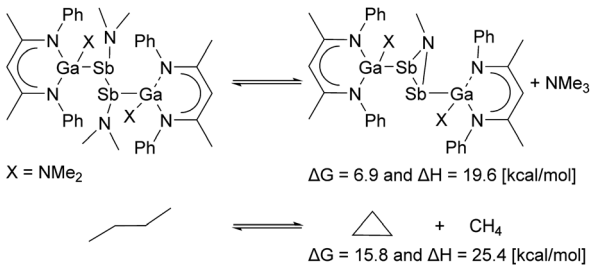

Scheme 5 The ring strain was estimated on the PBE0(def2-TZVP/D3BJ) level of theory with the isodesmic model reaction of a bisdimethylamido-substituted distibane to dimethylamine substituted azadistibirane. For comparison the analog method was applied to cyclopropane yielding 25.4 kcal mol^{-1}, which is close to the accepted value of 27.5 kcal mol^{-1}.[24]

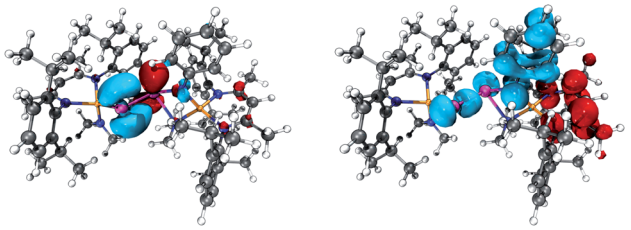

Fig. 3 Depiction of the electron difference density of the ground and excited state of the dominant 4th (left 456 nm) and 3rd (right 463 nm) excitation calculated by tddft [L(Me_2N)GaSbSbN(Ph)Ga(NMe_2)L] (**5**), blue hole and red accumulation.[23]

To the best of our knowledge, distibenes **4**, **5** and **8** represent the only structurally characterized heteroleptic distibenes. The LUMO of distibenes is typically represented by a low-lying π* orbital, whereas the level of the molecular orbitals of the π orbitals are somewhat indistinct since their energy levels are close to those of n_+ orbital.[5c,15] In contrast, both the π and σ Sb–Sb orbitals of **4** and **5** correspond to the HOMO and HOMO−1, respectively (Fig. S59†), whereas the LUMO is centered at the β-diketiminate ligand and the LUMO+1 is Sb-centred. In addition, these orbitals are significantly polarized towards the Ga-substituted Sb atom. Interestingly for the bisamido-substituted distibene **10** the LUMO is also Sb-centred (Fig. 2).

The bonding nature was further analysed by natural population analysis (NPA, Table S3†).[22] Compared to [L(Me_2N)GaSb]$_2$ (−0.16 *e*) the natural charge on the Ga-substituted Sb atom decreased (−0.69 **4**, −0.66 *e* **5**) while the charge on the amido-substituted Sb atom increased (1.05 **4**, 1.08 *e* **5**), respectively. The charge is even higher than that of distibene **10** (0.63 *e*). The π-bond is analogously polarized (occupation numbers (ON) π 1.89 *e* (**4**), ON π 1.89 *e* (**5**) with 71.9% and 71.1% polarization towards the Ga-substituted Sb atom), and the positively polarized Sb atom enables the dative interaction of the NMe_2 group. The Wiberg bond order (WBI) of the Sb–NMe_2 bond is roughly half of that of the Sb–NR bond (0.22, 0.49 **4**; 0.21, 0.49 **5**). Second order perturbation theory analysis revealed that the main interaction is the donation of the N-LP (lone pair) into the Sb–Sb π* orbital (21 kcal mol^{-1} **4** and **5**), which most likely is the main driving force for the ring opening together with the ring strain (Scheme 5).

In addition, TDDFT calculations of **4**, **5** and **10** were performed and compared to experimental UV-Vis-data (Table S2†). As was reported for [L(Me_2N)GaSb]$_2$,[10a] one dominant transition at 563 nm was found for **10** (Fig. S62†), which fits nicely to the experimental data. 87% of the transition orbitals comprise of the HOMO and LUMO orbitals, corresponding to known π → π* transition for distibenes.[15] Four and two transitions in the visible region of similar intensity and energy were found for **4** (Fig. S60†) and **5** (Fig. S61†), which are blue shifted compared to experimental values. The HOMO and LUMO+1 orbitals are the main contributions to the π → π* transition. Due to the polarized Sb–Sb double bond, the ground state is centred on the L(NMe_2)Ga-substituted Sb atom and the excited state on the RN-substituted Sb atom (Fig. 3). The HOMO−1 → LUMO transition contributes to the adsorption band of **4** and **5** in the visible region and can be regarded as metal-to-ligand charge transfer (MLCT) transition as the HOMO−1 (Fig. 2) correlates to the Sb–Sb σ-bond and the LUMO is ligand centred and correlates to C–N π*-bond of the β-diketiminate ligand.

The bonding situation of the three-membered rings was also investigated by the atoms in molecules approach (AIM, Tables S4 and S5).†[25] The nuclear attractors within the rings are connected to each other *via* bond paths. The Sb–Sb bond

 © 2022 The Author(s). Published by the Royal Society of Chemistry

Open Access Article. Published on 03 March 2022. Downloaded on 10/28/2025 3:34:55 PM.
This article is licensed under a Creative Commons Attribution-NonCommercial 3.0 Unported Licence.

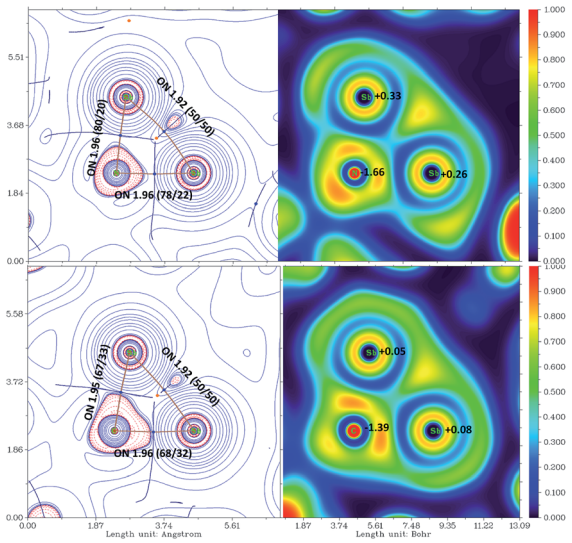

Fig. 4 Contour maps of the Laplacian of the electron density (left negative values red, positive blue), bond paths (brown), bcp (light blue), rcp (orange) and basin boundaries (dark blue) are indicated and ELF distribution (right), in the Sb–X–Sb plane of $[L(Me_2N)GaSb]_2NSiMe_3$ (**16**) (top) and $[L(Me_2N)GaSb]_2C(H)SiMe_3$ (**11**) (bottom). Occupation numbers (ON, |*e*|) of the σXY bonds according to NBO analysis with squared polarization coefficients and the natural charge is given.

is significantly bent outwards as indicated by ELF distribution (see Fig. 4).[26] The ring atoms are connected by polarized σ-bond (NBO) with occupation numbers close to two. NHO directionality and bond bending analysis showed high deviation from the line connecting the nuclear centers (Sb–Sb 33.7°). In contrast, the electron concentration of the C/N–Sb bond is within the spanned triangle and the ring critical point (RCP) is in proximity to the bond critical point (BCP) of the Sb–Sb bond.

Conclusion

L(X)Ga-substituted distibenes react with organoazides RN_3 (R: Ph **1**, *p*-CF_3Ph **2**, ada **3**) and $Me_3Si(H)CN_2$ in [2 + 1] cycloaddition reactions to azadistibiranes **1–3** and distibiranes **11–13** (X = NMe_2 **11**, OEt **12**, Cl **13**). While cycloaddition reactions are known for diphosphenes, analogous reactions of the heavier group 15 congeners are virtually unknown. Azadistibiranes **1–3** rearrange upon heating to heteroleptic distibenes, formally *via* insertion of the nitrene unit into the Ga–Sb bond (**5**, **6**), which occurred directly in the reaction with Me_3SiN_3 (**4**).

5 furthermore reacts with a second equivalent of PhN_3 to unsymmetric azadistibirane **9**, which isomerizes at elevated temperature to the homoleptic distibene **10**. In addition, the [2 + 2] cycloaddition of **5** yields tetrastibacyclobutane **7**. Heteroleptic distibenes **4** and **5** showed smaller π–π* gaps compared to the homoleptic distibene $[L(Me_2N)GaSb]_2$ according to UV-Vis measurements, and quantum chemical calculations suggest strongly polarized Sb–Sb double bonds. In addition, the π-donating N(R)Ga unit raises the energy of the Sb–Sb bonding orbitals. The HOMO and HOMO−1 correspond to the Sb–Sb bonding π and σ orbitals of **4**, **5** and **10**, rendering them attractive candidates for the synthesis of unknown distibene radical cations, which is currently under investigation.

Experimental

General procedures

All manipulations were carried out using standard Schlenk and glovebox techniques under argon, which was dried by passing through pre-heated Cu_2O pellets and molecular sieve columns. Toluene, *n*-pentane and *n*-hexane were dried with a MBraun Solvent Purification System, while benzene and deuterated solvents (toluene-d_8, C_6D_6) were distilled from Na/K alloy, and CH_3CN was distilled from CaH_2. All solvents were degassed and stored over activated molecular sieves. $[L(Cl)GaSb]_2$,[9b] $[L(EtO)GaSb]_2$,[9d] and $[L(Me_2N)GaSb]_2$ [9a] were prepared according to literature methods. Methyl *tert*-butyl ether (MTBE) solutions of PhN_3 and *p*-CF_3PhN_3 were stored over activated molecular sieves (4 Å) at −30 °C for one week prior to use. ^{1}H (300 MHz, 400 MHz, 600 MHz), $^{13}C\{^1H\}$ (100.7 MHz, 150.9 MHz), ^{19}F (282.3 MHz, 376.5 MHz, 564.6 MHz) and ^{29}Si (79.5 MHz, 119.2 MHz) NMR spectra were recorded using a Bruker Avance DPX-300, a Bruker Avance Neo 400 MHz or a Bruker Avance III HD 600 spectrometer and referenced to internal C_6D_5H (^{1}H: δ = 7.16; ^{13}C: δ = 128.06) or $C_6D_5CD_2H$ (^{1}H: δ = 2.08; ^{13}C: δ = 20.43). Assignment of the resonances was aided by 2D NMR spectroscopy. IR spectra were recorded in a glovebox using a BRUKER ALPHA-T FT-IR spectrometer equipped with a single reflection ATR sampling module. Microanalyses were performed at the elemental analysis laboratory of the University of Duisburg-Essen. UV-Vis-spectra were recorded on a Shimadzu UV-2600i spectrophotometer in a closed glass cuvette (10 mm) under argon atmosphere.

Caution! Me_3SiN_3 should be handled with caution under anhydrous conditions in an inert atmosphere or in a well-ventilated fume hood, as hydrolysis can lead to formation of toxic HN_3. Azide reactions should generally be performed in small scales.

$[L(Me_2N)GaSb]_2NPh$ (1). $[L(Me_2N)GaSb]_2$ (250 mg, 191 μmol) was suspended in 10 ml of toluene. 383 μl of a PhN_3 solution, 0.5 M in MTBE, was diluted with 2 ml of toluene and added dropwise to the suspension at −30 °C. The suspension was stirred for 12 h and the resulting solution stored at −30 °C for 24 h, yielding a red powder that was filtered off (165 mg). The filtrate was concentrated to 0.5 ml and stored at −30 °C, yielding another fraction (65 mg) of **1**. Yield: 215 mg (154 μmol, 80%). Anal. calcd for $C_{68}H_{99}Ga_2N_7Sb_2$: C, 58.44; H, 7.14; N, 7.02%. Found: C, 58.4; H, 7.10 N, 6.59%. ATR-IR: ν 3050, 2951, 2853, 2742, 1574, 1539, 1517, 1457, 1431, 1380, 1355, 1310, 1250, 1171, 1095, 1013, 962, 852, 791, 754, 743, 727, 681, 542, 437 cm^{-1}. ^{1}H NMR (400 MHz, C_6D_6, 25 °C): δ 7.24–6.99 (m, 12H, C_6H_3-2,6^{i}Pr$_2$), 6.74–6.66 (m, 3H, N–C_6H_5), 5.28 (m, 2H, N–C_6H_5), 4.66 (s, 2H, γ-CH), 3.61 (sept, $^3J_{HH}$ = 6.9 Hz, 2H, $CH(CH_3)_2$), 3.46 (sept, $^3J_{HH}$ = 6.8 Hz, 2H, $CH(CH_3)_2$), 3.29 (sept, $^3J_{HH}$ = 6.8 Hz, 2H, $CH(CH_3)_2$), 3.14 (sept, $^3J_{HH}$ = 6.8 Hz, 2H, $CH(CH_3)_2$), 2.70 (s(br), 6H, $N(CH_3)_2$), 2.24 (s(br), 6H, $N(CH_3)_2$), 1.62 (d, $^3J_{HH}$ = 6.8 Hz, 6H, $CH(CH_3)_2$), 1.52 (s, 6H, $ArNCCH_3$), 1.50 (s, 6H,

Open Access Article. Published on 03 March 2022. Downloaded on 10/28/2025 3:34:55 PM. This article is licensed under a Creative Commons Attribution-NonCommercial 3.0 Unported Licence.

ArNCCH$_3$), δ 1.40 (d, $^3J_{HH}$ = 6.7 Hz, 6H, CH(CH$_3$)$_2$), 1.35 (d, $^3J_{HH}$ = 7.0 Hz, 6H, CH(CH$_3$)$_2$), 1.27 (d, $^3J_{HH}$ = 6.8 Hz, 6H, CH(CH$_3$)$_2$), 1.19 (d, $^3J_{HH}$ = 6.7 Hz, 6H, CH(CH$_3$)$_2$), 1.17 (d, $^3J_{HH}$ = 6.8 Hz, 6H, CH(CH$_3$)$_2$), 1.09 (d, $^3J_{HH}$ = 6.7 Hz, 6H, CH(CH$_3$)$_2$), 0.99 (d, $^3J_{HH}$ = 6.7 Hz, 6H, CH(CH$_3$)$_2$). ^{13}C NMR (100.6 MHz, C$_6$D$_6$): δ 168.6, 168.3 (ArNCCH$_3$), 157.9 (N–C$_6$H$_5$), 145.8, 145.3, 142.9, 142.2, 127.4, 127.2, 125.9, 124.6, 124.5, 124.2 (ArC), 129.7, 125.2, 117.1 (N–C$_6$H$_5$), 96.8 (γ-CH), 45.5, 45.2 (N(CH$_3$)$_2$), 30.4, 29.3, 28.0, 27.9 (CH(CH$_3$)$_2$), 26.1, 26.0, 25.8, 25.3, 25.2, 25.0, 24.8, 24.6 (CH(CH$_3$)$_2$), 23.8, 23.7. (ArNCCH$_3$).

[L(Me$_2$N)GaSb]$_2$N(p-CF$_3$Ph) (2). 153 μl of a p-CF$_3$–PhN$_3$ solution (0.5 M in MTBE) was diluted with 0.5 ml of toluene and dropwise added at −30 °C to a suspension of [L(Me$_2$N)GaSb]$_2$ (100 mg, 76.5 μmol) in 5 ml of toluene. Stirring for 16 h at −30 °C gave a red solution, which was layered with 10 ml of *n*-hexane and stored at −30 °C, resulting in the precipitation of an orange solid that was isolated by filtration. Yield: 50 mg (34 μmol, 45%). Anal. calcd for C$_{69}$H$_{98}$F$_3$Ga$_2$N$_7$Sb$_2$: C, 56.55; H, 6.74 N, 6.69. Found: C, 56.4; H, 7.16; N, 6.37%. ATR-IR: ν 050, 2951, 2856, 2742, 1593, 1539, 1513, 1457, 1430, 1387, 1355, 1310, 1267, 1252, 1171, 1099, 1088, 1055, 1013, 965, 931, 852, 814, 793, 754, 724, 640, 542, 434 cm^{-1}. ^{1}H NMR (400 MHz, C$_6$D$_6$, 25 °C): δ 7.23–7.00 (m, 12H, C$_6$H$_3$-2,6^{i}Pr$_2$ and 2H, N–C$_6$H$_4$–CF$_3$), 5.11 (m, 2H, N–C$_6$H$_4$–CF$_3$), 4.64 (s, 2H, γ-CH), δ 3.58 (sept, $^3J_{HH}$ = 6.7 Hz, 2H, CH(CH$_3$)$_2$), 3.40 (sept, $^3J_{HH}$ = 6.8 Hz, 2H, CH(CH$_3$)$_2$), 3.28 (sept, $^3J_{HH}$ = 6.8 Hz, 2H, CH(CH$_3$)$_2$), 3.07 (sept, $^3J_{HH}$ = 6.8 Hz, 2H, CH(CH$_3$)$_2$), 2.64 (s(br), 6H, N(CH$_3$)$_2$), 2.21 (s(br), 6H, N(CH$_3$)$_2$), 1.60 (d, $^3J_{HH}$ = 6.9 Hz, 6H, CH(CH$_3$)$_2$), 1.48 (s, 6H, ArNCCH$_3$), 1.47 (s, 6H, ArNCCH$_3$), δ 1.35 (d, $^3J_{HH}$ = 6.6 Hz, 6H, CH(CH$_3$)$_2$), 1.33 (d, $^3J_{HH}$ = 6.9 Hz, 6H, CH(CH$_3$)$_2$), 1.25 (d, $^3J_{HH}$ = 6.8 Hz, 6H, CH(CH$_3$)$_2$), 1.17 (d, $^3J_{HH}$ = 6.7 Hz, 6H, CH(CH$_3$)$_2$), 1.11 (d, $^3J_{HH}$ = 6.9 Hz, 6H, CH(CH$_3$)$_2$), 1.07 (d, $^3J_{HH}$ = 6.7 Hz, 6H, CH(CH$_3$)$_2$), 0.92 (d, $^3J_{HH}$ = 6.6 Hz, 6H, CH(CH$_3$)$_2$). Resonance only observed in 2D NMR highlighted in italics. ^{13}C NMR (100.6 MHz, C$_6$D$_6$): δ 168.9, 168.5 (ArNCCH$_3$), 162.0 (N–C$_6$H$_5$–CF$_3$), 146.0, 145.4, 142.8, 142.7, 142.6, 142.0, 127.4, 126.1, 125.7, 124.7, 124.5, 124.2 (ArC), 129.3, 124.0, 117.9 (N–C$_6$H$_5$–CF$_3$), 96.9 (γ-CH), 45.3, 45.3 (N(CH$_3$)$_2$), 30.4, 29.4, 28.0, 27.9 (CH(CH$_3$)$_2$), 26.0, 26.0, 25.4, 25.2, 25.2, 25.0, 24.7, 24.6 (CH(CH$_3$)$_2$), 23.7, 23.7. (ArNCCH$_3$). ^{19}F NMR (376.5 MHz, C$_6$D$_6$): δ −59.5 (N–C$_6$H$_5$–CF$_3$).

[L(Me$_2$N)GaSb]$_2$N(ada) (3). [L(Me$_2$N)GaSb]$_2$ (200 mg, 153 μmol) were suspended in 5 ml of toluene and 26.3 mg of 1-ada-N$_3$ (153 μmol) dissolved in 2 ml of toluene was added to suspension at 0 °C over the course of 1 h. The suspension was stirred for 12 h, resulting in a dark red solution, which was evaporated to dryness and 20 ml of *n*-hexane were added. 10 mg of unreacted [L(Me$_2$N)GaSb]$_2$ was separated by filtration. The filtrate was concentrated to 0.3 ml and stored at −30 °C, yielding a dark red solid. Pure **3** was precipitated from a toluene solution after slow diffusion of CH$_3$CN at ambient temperature. Yield: 40 mg (27 μmol, 18%). ATR-IR: ν 3050, 2951, 2888, 2749, 1539, 1517, 1431, 1387, 1355, 1310, 1252, 1169, 1092, 1083, 1053, 1013, 963, 791, 754, 725, 542, 526, 437 cm^{-1}. ^{1}H NMR (600 MHz, C$_6$D$_6$, 25 °C): δ 7.31 (t, $^3J_{HH}$ = 7.7 Hz, 2H, C$_6$H$_3$-2,6^{i}Pr$_2$), 7.18–7.13 (m, 2H, C$_6$H$_3$-2,6^{i}Pr$_2$), 7.09–7.05 (m, 6H, C$_6$H$_3$-2,6^{i}Pr$_2$), 4.74 (s, 2H, γ-CH), 3.79 (sept, $^3J_{HH}$ = 6.9 Hz, 2H, CH(CH$_3$)$_2$), 3.53 (sept, $^3J_{HH}$ = 6.8 Hz, 2H, CH(CH$_3$)$_2$), 3.43 (sept, $^3J_{HH}$ = 6.8 Hz, 2H, CH(CH$_3$)$_2$), 3.30 (sept, $^3J_{HH}$ = 6.8 Hz, 2H, CH(CH$_3$)$_2$), 2.88 (s, 6H, N(CH$_3$)$_2$), 2.61 (s, 6H, N(CH$_3$)$_2$), 1.80–1.77 (m, 3H, 1-ada-CH), 1.58 (d, $^3J_{HH}$ = 6.9 Hz, 6H, CH(CH$_3$)$_2$), 1.55 (d, $^3J_{HH}$ = 6.9 Hz, 6H, CH(CH$_3$)$_2$), 1.50 (s, 6H, ArNCCH$_3$), 1.47 (s, 6H, ArNCCH$_3$), 1.38 (d, $^3J_{HH}$ = 6.7 Hz, 6H, CH(CH$_3$)$_2$), 1.32 (dd, $^3J_{HH}$ = 13.1 Hz 6H, 1-ada-CH$_2$), 1.32 (d, $^3J_{HH}$ = 6.7 Hz, 6H, CH(CH$_3$)$_2$), 1.23 (d, $^3J_{HH}$ = 6.8 Hz, 12H, CH(CH$_3$)$_2$), 1.19 (d, $^3J_{HH}$ = 6.7 Hz, 6H, CH(CH$_3$)$_2$), δ 1.09 (d, $^3J_{HH}$ = 6.7 Hz, 6H, CH(CH$_3$)$_2$), 0.85–0.75 (m, 6H, 1-ada-CH$_2$). ^{13}C NMR (151 MHz, C$_6$D$_6$) δ 168.3, 168.2 (ArNCCH$_3$), 145.2, 145.2, 144.0, 143.3, 142.8, 142.6, 127.5, 127.1, 125.4, 125.3, 124.2, 123.9 (ArC), 97.5 (γ-CH), 51.9 (1-ada-NC), 51.0 (1-ada-NCH$_2$), 46.3, 45.2 (N(CH$_3$)$_2$), 37.0 (1-ada-NCH$_2$), 31.6 (1-ada-NCH), 30.1, 29.4, 28.0, 27.9, (CH(CH$_3$)$_2$), 27.2, 25.4, 25.4, 25.4, 25.3, 25.0, 24.7, 24.4 (CH(CH$_3$)$_2$), 23.9, 23.8 (ArNCCH$_3$).

L(Me$_2$N)GaSbSbN(SiMe$_3$)Ga(NMe$_2$)L (4). [L(Me$_2$N)GaSb]$_2$ (100 mg, 77 μmol) was suspended in 5 ml of toluene and 11.07 μl (8.8 mg, 77 μmol) of Me$_3$SiN$_3$ diluted in 20 ml toluene was added dropwise within 1.5 h at −10 °C. The reaction mixture was stirred for 12 h at ambient temperature, the dark red solution was evaporated to dryness and 5 ml of *n*-hexane added. 20 mg of unreacted [L(Me$_2$N)GaSb]$_2$ was separated by filtration, the filtrate concentrated to 0.5 ml and stored at −30 °C, yielding 47 mg of red crystalline solid. Yield: 47 mg (44%). Anal. calcd for C$_{65}$H$_{103}$Ga$_2$N$_7$Sb$_2$Si: C, 56.02; H, 7.45; N, 7.04%. Found: C, 55.8; H, 7.23; N 6.85%. ATR-IR: ν 3046, 2950, 2853, 2747, 1540, 1516, 1456, 1431, 1378, 1355, 1310, 1250, 1235, 1171, 1015, 963, 932, 912, 872, 853, 827, 791, 754, 627, 605, 529, 439 cm^{-1}. ^{1}H NMR (600 MHz, C$_6$D$_6$, 25 °C): δ 7.16 (dd, $^3J_{HH}$ = obscured by C$_6$D$_5$H, $^4J_{HH}$ = 2.1 Hz, 2H, C$_6$H$_3$-2,6^{i}Pr$_2$), 7.14 (t, $^3J_{HH}$ = 7.4 Hz, 2H, C$_6$H$_3$-2,6^{i}Pr$_2$), 7.11 (m, 4H, C$_6$H$_3$-2,6^{i}Pr$_2$), 7.05 (t, $^3J_{HH}$ = 7.6 Hz, 2H, C$_6$H$_3$-2,6^{i}Pr$_2$), 6.94 (dd, $^3J_{HH}$ = 7.6 Hz, $^4J_{HH}$ = 1.6 Hz, 2H, C$_6$H$_3$-2,6^{i}Pr$_2$), 4.89 (s, 1H, γ-CH), 4.77 (s, 1H, γ-CH), 3.97 (sept, $^3J_{HH}$ = 6.6 Hz, 2H, CH(CH$_3$)$_2$), 3.73 (sept, $^3J_{HH}$ = 6.8 Hz, 2H, CH(CH$_3$)$_2$), 3.56 (sept, $^3J_{HH}$ = 6.9 Hz, 2H, CH(CH$_3$)$_2$), 3.23 (s, 3H, N(CH$_3$)$_2$), 3.01 (sept, $^3J_{HH}$ = 6.8 Hz, 2H, CH(CH$_3$)$_2$), 2.90 (s, 3H, N(CH$_3$)$_2$), 1.94 (s, 6H, N(CH$_3$)$_2$), 1.69 (s, 6H, ArNCCH$_3$), 1.58 (d, $^3J_{HH}$ = 6.8 Hz, 6H, CH(CH$_3$)$_2$), 1.53 (d, $^3J_{HH}$ = 6.7 Hz, 6H, CH(CH$_3$)$_2$), 1.41 (d, $^3J_{HH}$ = 6.7 Hz, 6H, CH(CH$_3$)$_2$), 1.33 (d, $^3J_{HH}$ = 6.9 Hz, 6H, CH(CH$_3$)$_2$), 1.30 (s, 6H, ArNCCH$_3$), 1.21 (d, $^3J_{HH}$ = 6.7 Hz, 12H, CH(CH$_3$)$_2$), 1.18 (d, $^3J_{HH}$ = 6.8 Hz, 6H, CH(CH$_3$)$_2$), 0.97 (d, $^3J_{HH}$ = 6.7 Hz, 6H, CH(CH$_3$)$_2$), 0.41 (s, 9H, NSi(CH$_3$)$_3$). ^{13}C NMR (151 MHz, C$_6$D$_6$): δ 170.9, 167.4 (ArNCCH$_3$), 145.5, 145.3, 143.9, 143.6, 143.0, 142.7, 128.0, 126.6, 125.7, 124.5, 124.4, 124.3 (ArC), 99.6, 96.8 (γ-CH), 45.3, 45.0, 44.1 (N(CH$_3$)$_2$), 29.6, 28.9, 28.0 27.6, (CH(CH$_3$)$_2$), 27.8, 26.5, 26.0, 25.3, 25.3, 25.1, 25.0 (CH(CH$_3$)$_2$), 24.4. (ArNCCH$_3$), 6.1 (CHSi(CH$_3$)$_3$). ^{29}Si NMR (79.5 MHz, C$_6$D$_6$, 25 °C): δ −4.5 (CHSi(CH$_3$)$_3$).

[L(Me$_2$N)GaSbSbN(Ph)Ga(NMe$_2$)L] (5). **1** (300 mg, 215 μmol) was suspended in 10 ml of toluene and stirred for 12 h at 80 °C, upon which the color changed from orange to purple. All volatiles were removed *in vacuo* and 10 ml of *n*-hexane was added. Small amounts of solids were separated by filtration. The filtrate was concentrated and stored add −30 °C to afford 205 mg of **5** as purple powder, which was obtained as slightly impure material despite several recrystallization experiments, hence no accurate

 © 2022 The Author(s). Published by the Royal Society of Chemistry

Open Access Article. Published on 03 March 2022. Downloaded on 10/28/2025 3:34:55 PM. This article is licensed under a Creative Commons Attribution-NonCommercial 3.0 Unported Licence.

elemental analysis were obtained. Yield: 215 mg (154 μmol, 72%). ATR-IR: ν 3047, 2947, 2915, 2854, 2744, 1579, 1517, 1456, 1431, 1378, 1355, 1311, 1278, 1248, 1172, 1094, 1014, 962, 930, 872, 791, 754, 724, 688, 510, 439 cm^{-1}. ^{1}H NMR (400 MHz, C_6D_6, 25 °C): δ 7.34 (m, 2H, N–C_6H_5), 7.24–6.95 (m, 12H, C_6H_3-2,6^{i}Pr$_2$), 6.74 (m, 1H, N–C_6H_5), 6.59 (m, 2H, N–C_6H_5), 4.94 (s, 1H, γ-CH), 4.90 (s, 1H, γ-CH), 3.73 (sept, $^3J_{HH}$ = 6.7 Hz, 1H, CH(CH$_3$)$_2$), 3.58 (sept, $^3J_{HH}$ = 6.8 Hz, 1H, CH(CH$_3$)$_2$), 3.28 (sept, $^3J_{HH}$ = 6.8 Hz, 1H, CH(CH$_3$)$_2$), 3.23 (s(br), 3H, N(CH$_3$)$_2$), 3.03 (sept, $^3J_{HH}$ = 6.8 Hz, 2H, CH(CH$_3$)$_2$), 2.88 (s(br), 3H, N(CH$_3$)$_2$), 1.90 (s, 6H, N(CH$_3$)$_2$), 1.72 (s, 6H, ArNCCH$_3$), 1.60 (d, $^3J_{HH}$ = 6.9 Hz, 6H, CH(CH$_3$)$_2$), 1.41 (s, 6H, N(CH$_3$)$_2$), 1.41 (d, $^3J_{HH}$ = 6.8 Hz, 6H, CH(CH$_3$)$_2$), 1.34 (d, $^3J_{HH}$ = 6.8 Hz, 6H, CH(CH$_3$)$_2$), 1.26 (d, $^3J_{HH}$ = 6.7 Hz, 6H, CH(CH$_3$)$_2$), 1.24 (d, $^3J_{HH}$ = 6.7 Hz, 6H, CH(CH$_3$)$_2$), 1.18 (d, $^3J_{HH}$ = 6.7 Hz, 6H, CH(CH$_3$)$_2$), 0.97 (d, $^3J_{HH}$ = 6.8 Hz, 6H, CH(CH$_3$)$_2$), 0.91 (d, $^3J_{HH}$ = 6.7 Hz, 6H, CH(CH$_3$)$_2$). ^{13}C NMR (100.6 MHz, C_6D_6): δ 170.9, 167.4 (ArNCCH$_3$), 155.7 (N–C_6H_5), 146.0, 145.3, 143.8, 143.6, 142.3, 141.4, 127.9, 126.6, 125.7, 124.6, 124.3, 123.7 (ArC), 128.2, 121.7, 113.9 (N–C_6H_5), 97.2, 96.7 (γ-CH), 45.3, 45.2, 44.0 (N(CH$_3$)$_2$), 29.7, 29.4, 28.1, 27.6 (CH(CH$_3$)$_2$), 26.9, 26.4, 25.8, 25.4, 25.1, 25.0, 24.8, 23.9 (CH(CH$_3$)$_2$), 24.4, 23.9 (ArNCCH$_3$).

L(Me$_2$N)GaSbSbN(p-CF$_3$Ph)Ga(NMe$_2$)L (6). **2** (150 mg, 102 μmol) was suspended in 2 ml of toluene and stirred at 100 °C for 2 h, upon which the color changed from orange to dark red. All volatiles were removed *in vacuo*, 4 ml of *n*-hexane was added and a small amount of an insoluble solid was separated by filtration. The filtrate was concentrated and stored add −30 °C to afford 110 mg of **6** as dark red powder which was slightly contaminated with **2**, but longer reaction times resulted in significantly reduced yield. Yield: 88 mg (60 μmol). Anal. calcd for $C_{69}H_{98}F_3Ga_2N_7Sb_2$: C, 56.55; H, 6.74; N, 6.69%. Found: C, 56.7; H, 6.64; N, 6.98%. ATR-IR: ν 3051, 2951, 2915, 2857, 2744, 1598, 1543, 1516, 1456, 1431, 1383, 1357, 1311, 1284, 1251, 1172, 1149, 1095, 1059, 1015, 963, 930, 855, 820, 791, 756, 723, 644, 617, 581, 526, 510, 439, 407 cm^{-1}. ^{1}H NMR (400 MHz, C_6D_6, 25 °C): δ 7.67 (d, $^3J_{HH}$ = 8.4 Hz, 2H, N–$C_6H_4CF_3$), 7.22–7.95 and 6.98–6.93 (m, 10H, C_6H_3-2,6^{i}Pr$_2$), 6.86 (dd, $^3J_{HH}$ = 6.7 Hz, $^4J_{HH}$ = 2.6 Hz, 2H, C_6H_3-2,6^{i}Pr$_2$), 6.57 (d, $^3J_{HH}$ = 8.4 Hz, 2H, N–$C_6H_4CF_3$), 4.91 (s, 1H, γ-CH), 4.87 (s, 1H, γ-CH), 3.69 (sept, $^3J_{HH}$ = 6.7 Hz, 1H, CH(CH$_3$)$_2$), 3.51 (sept, $^3J_{HH}$ = 6.8 Hz, 1H, CH(CH$_3$)$_2$), 3.19 (s, 3H, N(CH$_3$)$_2$), 3.10 (sept, $^3J_{HH}$ = 6.8 Hz, 1H, CH(CH$_3$)$_2$), 2.98 (sept, $^3J_{HH}$ = 6.8 Hz, 2H, CH(CH$_3$)$_2$), 2.84 (s, 3H, N(CH$_3$)$_2$), 1.84 (s, 6H, N(CH$_3$)$_2$), 1.69 (s, 6H, ArNCCH$_3$), 1.54 (d, $^3J_{HH}$ = 6.9 Hz, 6H, CH(CH$_3$)$_2$), 1.38 (d, $^3J_{HH}$ = 6.6 Hz, 6H, CH(CH$_3$)$_2$), 1.37 (s, 6H, N(CH$_3$)$_2$), 1.32 (d, $^3J_{HH}$ = 6.8 Hz, 6H, CH(CH$_3$)$_2$), 1.19 (d, $^3J_{HH}$ = 6.8 Hz, 6H, CH(CH$_3$)$_2$), 1.18 (d, $^3J_{HH}$ = 6.7 Hz, 6H, CH(CH$_3$)$_2$), 1.16 (d, $^3J_{HH}$ = 6.7 Hz, 6H, CH(CH$_3$)$_2$), 0.95 (d, $^3J_{HH}$ = 6.7 Hz, 6H, CH(CH$_3$)$_2$), 0.85 (d, $^3J_{HH}$ = 6.7 Hz, 6H, CH(CH$_3$)$_2$). ^{13}C NMR (100.6 MHz, C_6D_6): δ 171.2, 167.6 (ArNCCH$_3$), 145.7, 145.3, 143.7, 143.6, 142.2, 141.1, 126.7, 125.7, 124.6, 124.3, 123.8, 121.2 (ArC), 97.2, 96.8 (γ-CH), 45.2, 45.1, 44.0 (N(CH$_3$)$_2$), 29.7, 29.4, 28.0, 27.6 (CH(CH$_3$)$_2$), 26.8, 26.3, 25.8, 25.4, 25.0, 24.9, 24.7, 23.8 (CH(CH$_3$)$_2$), 24.4, 23.9, (ArNCCH$_3$). ^{19}F NMR (282.4 MHz, C_6D_6): δ −59.3 (N–C_6H_5–CF$_3$).

(L(PhN)Ga-κGa,κN)$_2$-(μ,η$^{1:1:1:1}$-Sb$_4$) (7). **1** (75 mg, 54 μmol) was suspended in 0.5 ml of toluene-d$_8$ and kept at 100 °C in a *J*-Young NMR-tube until initially formed **5** was converted to an orange solid, which was isolated and recrystallized from 10 ml of hot toluene. Yield: 13 mg (8 μmol, 29%). Anal. calcd for C, 51.14; H, 5.64; N, 5.11%. Found: C, 51.1; H, 5.93; N, 4.79%. ATR-IR: ν 3044, 2947, 2912, 2854, 1575, 1520, 1457, 1430, 1388, 1378, 1355, 1310, 1250, 1172, 1017, 981, 857, 790, 726, 681, 597, 523 cm^{-1}. 1.66 (s, 6H), 1.46 (d, J = 3.1 Hz, 3H), 1.44 (d, J = 3.2 Hz, 3H), 1.13 (d, J = 6.6 Hz, 3H), 1.08 (d, J = 3.2 Hz, 3H), 1.06 (d, J = 3.2 Hz, 3H), 0.97 (dd, J = 6.8, 1.4 Hz, 11H). ^{1}H NMR (300 MHz, C_6D_6, 70 °C): δ 7.28 (t, $^3J_{HH}$ = 6.7 Hz, 4H, C_6H_3-2,6^{i}Pr$_2$), 7.13–6.88 (m, 14H, C_6H_3-2,6^{i}Pr$_2$), 6.65 (t, $^3J_{HH}$ = 7.4 Hz, 2H, N–C_6H_5), 4.94 (s, 1H, γ-CH), δ 3.45 (sept, $^3J_{HH}$ = 6.6 Hz, 2H, CH(CH$_3$)$_2$), 3.27 (m, 6H, CH(CH$_3$)$_2$), δ 1.66 (s, 12H, ArNCCH$_3$), 1.46 (d, $^3J_{HH}$ = 6.8 Hz, 6H, CH(CH$_3$)$_2$), 1.44 (d, $^3J_{HH}$ = 6.8 Hz, 6H, CH(CH$_3$)$_2$), 1.13 (d, $^3J_{HH}$ = 6.6 Hz, 6H, CH(CH$_3$)$_2$), 1.08 (d, $^3J_{HH}$ = 6.7 Hz, 6H, CH(CH$_3$)$_2$), 1.07 (d, $^3J_{HH}$ = 6.8 Hz, 6H, CH(CH$_3$)$_2$), 0.97 (d(br), $^3J_{HH}$ = 6.8 Hz, 12H, CH(CH$_3$)$_2$). ^{13}C NMR spectra could not be obtained due to the low solubility.

L(Me$_2$N)GaSbSbN(SiMe$_3$)Ga(N(H)SiMe$_3$)L (8). [L(Me$_2$N)GaSb]$_2$ (300 mg, 223 μmol) was suspended in 10 ml of toluene and 62.5 μl (54 mg, 471 μmol) Me$_3$SiN$_3$ diluted in 20 ml of toluene was added dropwise within 1.5 h at −10 °C. The reaction mixture was stirred for 12 h at room temperature, and the resulting dark red solution was evaporated to dryness. 20 ml of *n*-hexane was added to the residue, all insoluble residues were removed by filtration. All volatiles were removed from the filtrate, which was then redissolved in 5 ml of toluene. **8** was isolated as dark-red crystalline solid after slow diffusion of CH$_3$CN into the toluene solution. Yield: 70 mg (21%). Anal. calcd for $C_{66}H_{107}Ga_2N_7Sb_2Si_2$: C, 55.14; H, 7.05; N, 6.82%. Found: C, 55.1; H, 6.95; N, 7.00%. ATR-IR: ν 3052, 2951, 2856, 2744, 1540, 1514, 1456, 1431, 1380, 1355, 1310, 1251, 1235, 1169, 1015, 968, 917, 870, 854, 829, 790, 771, 753, 623, 527, 433 cm^{-1}. ^{1}H NMR (600 MHz, C_6D_6, 25 °C): δ 7.15–7.06 (m, 12H, C_6H_3-2,6^{i}Pr$_2$), 4.89 (s, 1H, γ-CH), 4.48 (s, 1H, γ-CH), 3.82 (sept, $^3J_{HH}$ = 6.7 Hz, 2H, CH(CH$_3$)$_2$), 3.75 (sept, $^3J_{HH}$ = 6.8 Hz, 2H, CH(CH$_3$)$_2$), 3.35 (sept, $^3J_{HH}$ = 6.9 Hz, 2H, CH(CH$_3$)$_2$), 3.23 (s, 3H, N(CH$_3$)$_2$), 3.20 (sept, $^3J_{HH}$ = 6.8 Hz, 2H, CH(CH$_3$)$_2$), 2.89 (s, 3H, N(CH$_3$)$_2$), 1.69 (s, 6H, N(CH$_3$)$_2$), 1.50 (s, 6H, ArNCCH$_3$), 1.46 (d, $^3J_{HH}$ = 6.7 Hz, 6H, CH(CH$_3$)$_2$), 1.43 (d, $^3J_{HH}$ = 6.7 Hz, 6H, CH(CH$_3$)$_2$), 1.42 (d, $^3J_{HH}$ = 6.8 Hz, 6H, CH(CH$_3$)$_2$), 1.37 (d, $^3J_{HH}$ = 6.8 Hz, 6H, CH(CH$_3$)$_2$), 1.36 (d, $^3J_{HH}$ = 6.9 Hz, 6H, CH(CH$_3$)$_2$), 1.16 (d, $^3J_{HH}$ = 6.8 Hz, 6H, CH(CH$_3$)$_2$), 1.14 (d, $^3J_{HH}$ = 6.6 Hz, 6H, CH(CH$_3$)$_2$), 1.07 (d, $^3J_{HH}$ = 6.8 Hz, 6H, CH(CH$_3$)$_2$), 0.59 (s, 1.5H, 0.5 eq. ACN), 0.47 (s, 9H, NSi(CH$_3$)$_3$), −0.25 (s, 9H, NSi(CH$_3$)$_3$), −0.63 (s, 1H, NHSi(CH$_3$)$_3$). ^{13}C NMR (151 MHz, C_6D_6): δ 170.5, 168.3 (ArNCCH$_3$), 145.5, 145.3, 143.4, 143.3, 143.2, 142.1, 127.3, 127.0, 125.4, 124.7, 124.6, 124.4 (ArC), 97.0, 92.8 (γ-CH), 45.7, 44.2 (N(CH$_3$)$_2$), 29.7, 28.7, 28.1, 27.6 (CH(CH$_3$)$_2$), 26.9, 26.5, 26.0, 25.9, 25.6, 25.3, 25.1, 25.0 (CH(CH$_3$)$_2$), 25.5, 24.3 (ArNCCH$_3$), 9.0, 3.9 (CHSi(CH$_3$)$_3$), δ 0.1 (ACN). ^{29}Si NMR (119 MHz, C_6D_6, 25 °C): δ 1.8, −4.4 (CHSi(CH$_3$)$_3$).

[L(Me$_2$N)GaSb][L(Me$_2$N)GaN(Ph)Sb]NPh (9). **5** (30 mg 21.5 μmol) was dissolved in 0.5 ml of toluene-d$_8$ and 42.9 μl of a 0.5 M PhN$_3$ MTBE solution was added at −30 °C. The mixture was stored for 24 h at −30 °C, yielding an orange precipitate. All volatiles were removed under reduced pressure and the

Open Access Article. Published on 03 March 2022. Downloaded on 10/28/2025 3:34:55 PM. This article is licensed under a Creative Commons Attribution-NonCommercial 3.0 Unported Licence.

resulting solid dissolved in warm toluene (60 °C) and recrystallized at 7 °C. Yield: 12 mg (8 μmol, 38%). Anal. calcd for $C_{74}H_{104}Ga_2N_8Sb_2$ C_7H_8: C, 61.54; H, 7.14; N, 7.09%. Found: C, 61.4; H, 6.74; N, 7.06%. ATR-IR: ν 3047, 2947, 2915, 2854, 2744, 1579, 1517, 1456, 1431, 1378, 1355, 1311, 1278, 1248, 1172, 1094, 1014, 962, 930, 872, 791, 754, 724, 688, 510, 439 cm^{-1}. ^1H NMR (600 MHz, C_6D_6, 25 °C): δ 7.39 (dd, $^3J_{HH}$ = 5.7 Hz, $^4J_{HH}$ = 3.5 Hz, 1H, C_6H_3-2,6^{i}Pr$_2$), 7.25–7.19 (m, 6H, C_6H_3-2,6^{i}Pr$_2$), 7.06–7.01 (m, 3H, C_6H_3-2,6^{i}Pr$_2$), 7.03 (t, ^3J = 7.8 Hz, 2H, N–C_6H_5), 6.87 (t, ^3J = 7.2 Hz, 2H, C_6H_3-2,6^{i}Pr$_2$), 6.52 (d, ^3J = 7.7 Hz, 1H, C_6H_3-2,6^{i}Pr$_2$), 6.43 (t, ^3J = 7.4 Hz, 2H, N–C_6H_5), 6.33 (t, ^3J = 7.2 Hz, 1H, N–C_6H_5), 6.10 (d, ^3J = 7.7 Hz, 2H, N–C_6H_5), 5.93 (d, ^3J = 7.7 Hz, 2H, N–C_6H_5), 4.68 (s, 1H, γ-CH), 4.61 (s, 1H, γ-CH), 3.56 (sept, $^3J_{HH}$ = 6.6 Hz, 1H, CH(CH$_3$)$_2$), 3.56 (d sept, $^3J_{HH}$ = 6.8 Hz, 2H, CH(CH$_3$)$_2$), 3.32 (sept, $^3J_{HH}$ = 6.8 Hz, 1H, CH(CH$_3$)$_2$), 3.26 (sept, $^3J_{HH}$ = 6.8 Hz, 1H, CH(CH$_3$)$_2$), 3.16 (sept, $^3J_{HH}$ = 6.7 Hz, 1H, CH(CH$_3$)$_2$), 3.12 (sept, $^3J_{HH}$ = 6.8 Hz, 1H, CH(CH$_3$)$_2$), 3.06 (s, 3H, N(CH$_3$)$_2$), 2.78 (sept, $^3J_{HH}$ = 6.8 Hz, 1H, CH(CH$_3$)$_2$), 2.74 (s(br), 3H, N(CH$_3$)$_2$), 2.71 (s, 3H, N(CH$_3$)$_2$), 2.24 (s(br), 3H, N(CH$_3$)$_2$), 1.62 (d, $^3J_{HH}$ = 6.7 Hz, 6H, CH(CH$_3$)$_2$), 1.59 (s, 3H, ArNCCH$_3$), 1.57 (d, $^3J_{HH}$ = 6.9 Hz, 3H, CH(CH$_3$)$_2$), 1.52 (s, 3H, ArNCCH$_3$), 1.50 (d, $^3J_{HH}$ = 6.9 Hz, 3H, CH(CH$_3$)$_2$), 1.48 (s, 3H, ArNCCH$_3$), 1.46 (s, 3H, ArNCCH$_3$), 1.45 (d, $^3J_{HH}$ = 6.8 Hz, 3H, CH(CH$_3$)$_2$), 1.34 (d, $^3J_{HH}$ = 6.8 Hz, 3H, CH(CH$_3$)$_2$), 1.50 (d, $^3J_{HH}$ = 6.9 Hz, 3H, CH(CH$_3$)$_2$), 1.32 (d, $^3J_{HH}$ = 6.6 Hz, 3H, CH(CH$_3$)$_2$), 1.30 (d, $^3J_{HH}$ = 6.6 Hz, 3H, CH(CH$_3$)$_2$), 1.21 (d, $^3J_{HH}$ = 6.9 Hz, 3H, CH(CH$_3$)$_2$), 1.15 (d, $^3J_{HH}$ = 6.9 Hz, 3H, CH(CH$_3$)$_2$), 1.06 (d, $^3J_{HH}$ = 6.8 Hz, 3H, CH(CH$_3$)$_2$), 1.06 (d, $^3J_{HH}$ = 6.8 Hz, 3H, CH(CH$_3$)$_2$), 0.96 (d, $^3J_{HH}$ = 6.7 Hz, 3H, CH(CH$_3$)$_2$), 0.84 (d, $^3J_{HH}$ = 6.8 Hz, 6H, CH(CH$_3$)$_2$), 0.65 (d, $^3J_{HH}$ = 6.7 Hz, 3H, CH(CH$_3$)$_2$). ^{13}C NMR (150.9 MHz, C_6D_6): δ 170.1, 169.3, 168.3, 167.9 (ArNCCH$_3$), 153.8, 152.7 (N–C_6H_5), 145.6, 145.6, 145.4, 144.6, 143.7, 143.5, 143.1, 143.0, 142.7, 142.7, 142.3, 142.2 (ArC), 129.7, 129.3, 128.6, 127.6, 127.1, 127.0, 127.0, 126.6, 125.7, 125.7, 125.3, 125.1, 124.7, 124.2, 124.1, 124.0, 123.9, 123.9, 123.7, 120.4, 117.4 (N–C_6H_5 + ArC, signal overlayed by C_6D_6), 96.3, 96.0 (γ-CH), 44.8, 44.8, 43.5 (N(CH$_3$)$_2$), 30.1, 30.0, 29.1, 29.0 (CH(CH$_3$)$_2$), 28.3, 28.0, 27.9, 27.7, 27.0, 25.8, 25.5, 25.5, 25.2, 25.2, 25.2, 25.1, 25.1, 25.0, 24.8, 24.8, 24.5, 24.4, 24.3, 24.3 (CH(CH$_3$)$_2$), 24.0, 23.6, 23.6, 23.5 (ArNCCH$_3$).

[L(Me$_2$N)GaN(Ph)Sb]$_2$ (10). **9** (50 mg, 34 μmol) was suspended in 2 ml of toluene and stirred for 12 h at 70 °C, upon which the color changed from orange to dark blue. The resulting dark blue precipitated was isolated by filtration and washed with toluene.

Yield: 18 mg (12.1 μmol, 36%). Anal. calcd for $C_{74}H_{104}Ga_2N_8Sb_2$: C, 61.54; H, 7.14; N, 7.09%. Found: C, 59.7; H, 7.15; N, 7.27%. ATR-IR: ν 2953, 2920, 2815, 2792, 2750, 1542, 1516, 1457, 1427, 1391, 1313, 1254, 1213, 1172, 1013, 965, 933, 851, 787, 763, 751, 674, 590, 500 cm^{-1}. ^1H NMR (400 MHz, C_6D_6, 25 °C): δ 7.09–7.03 (m, 8H, C_6H_3-2,6^{i}Pr$_2$), 6.84 (dd, $^3J_{HH}$ = 7.2 Hz, $^4J_{HH}$ = 2.0 Hz, 4H, C_6H_3-2,6^{i}Pr$_2$), 6.69 (t, ^3J = 7.3 Hz, 4H, C_6H_3-2,6^{i}Pr$_2$), 6.61 (d, ^3J = 7.3 Hz, 4H, C_6H_3-2,6^{i}Pr$_2$), 6.50 (t, ^3J = 7.2 Hz, 2H, C_6H_3-2,6^{i}Pr$_2$), δ 4.61 (s, 2H, γ-CH), 3.35 (sept, $^3J_{HH}$ = 6.8 Hz, 2H, CH(CH$_3$)$_2$), 3.30 (sept, $^3J_{HH}$ = 6.8 Hz, 2H, CH(CH$_3$)$_2$), 2.88 (s, 6H, N(CH$_3$)$_2$), δ 2.84 (s, 6H, N(CH$_3$)$_2$), 1.48 (s, 12H, ArNCCH$_3$), 1.37 (d, $^3J_{HH}$ = 6.6 Hz, 12H, CH(CH$_3$)$_2$), 1.31 (d, $^3J_{HH}$ = 6.7 Hz, 12H, CH(CH$_3$)$_2$), 1.24 (d, $^3J_{HH}$ = 6.8 Hz, 12H, CH(CH$_3$)$_2$), 1.00 (d, $^3J_{HH}$ = 6.8 Hz, 12H, CH(CH$_3$)$_2$). DEPTQ ^{13}C NMR (150.9 MHz, C_6D_6): δ 169.2 (ArNCCH$_3$), 168.2 (N–C_6H_5), 144.3, 143.0, 142.8, 127.1, 124.4, 123.9 (ArC), 128.1, 123.3, 119.3 (N–C_6H_5), 95.5 (γ-CH), 43.8, 42.9 (N(CH$_3$)$_2$), 29.7, 29.4, 28.1, 27.6 28.7, 27.5 (CH(CH$_3$)$_2$), 25.0, 24.8, 24.4, 24.0 (CH(CH$_3$)$_2$), 23.5 (ArNCCH$_3$).

[L(Me$_2$N)GaSb]$_2$C(H)SiMe$_3$ (11). [L(Me$_2$N)GaSb]$_2$ (60 mg, 46 μmol) was suspended in 2 ml of toluene and 78.1 μl of a Me$_3$Si(H)CN$_2$ solution (0.6 M in *n*-hexane) was added. The suspension was stirred for 12 h at room temperature. Storing at 6 °C led to a first fraction of large orange crystals (45 mg), while a second fraction was isolated after concentration of the filtrate to 0.3 ml and storage at −6 °C. Yield: 58 mg (54 μmol, 90%). Anal. calcd for $C_{66}H_{104}Ga_2N_6Sb_2Si$ + C_7H_8: C, 59.05; H, 7.60; N, 5.66%. Found: C, 58.8; H, 7.75; N, 5.71%. ATR-IR: ν 3058, 2965, 2924, 2865, 2756, 1524, 1436, 1383, 1314, 1252, 1173, 1018, 965, 856, 794, 728, 694, 461 cm^{-1}. ^1H NMR (600 MHz, C_6D_6, 25 °C): δ 7.29–7.24 (m, 4H, C_6H_3-2,6^{i}Pr$_2$), 7.15–7.06 (m, 8H, C_6H_3-2,6^{i}Pr$_2$), 4.76 (s, 1H, γ-CH), 4.72 (s, 1H, γ-CH), 3.83 (sept, $^3J_{HH}$ = 6.8 Hz, 1H, CH(CH$_3$)$_2$), 3.51 (sept, $^3J_{HH}$ = 6.8 Hz, 1H, CH(CH$_3$)$_2$), 3.44 (sept, $^3J_{HH}$ = 6.8 Hz, 3H, CH(CH$_3$)$_2$), 3.38 (sept, $^3J_{HH}$ = 6.8 Hz, 1H, CH(CH$_3$)$_2$), 3.26 (sept, $^3J_{HH}$ = 6.8 Hz, 1H, CH(CH$_3$)$_2$), 3.16 (sept, $^3J_{HH}$ = 6.8 Hz, 1H, CH(CH$_3$)$_2$), 2.89 (s, 3H, N(CH$_3$)$_2$), 2.83 (s, 3H, N(CH$_3$)$_2$), 2.44 (s, 3H, N(CH$_3$)$_2$), 2.36 (s, 3H, N(CH$_3$)$_2$), 1.81 (s, 1H, CHSi(CH$_3$)$_3$), 1.63 (d, $^3J_{HH}$ = 6.9 Hz, 3H, CH(CH$_3$)$_2$), 1.59 (d, $^3J_{HH}$ = 6.9 Hz, 3H, CH(CH$_3$)$_2$), 1.54 (d, $^3J_{HH}$ = 7.4 Hz, 3H, CH(CH$_3$)$_2$), 1.53 (s, 3H, ArNCCH$_3$), 1.51 (s, 6H, ArNCCH$_3$), 1.49 (d, $^3J_{HH}$ = 6.9 Hz, 3H, CH(CH$_3$)$_2$), 1.48 (s, 3H, ArNCCH$_3$), 1.37 (d, $^3J_{HH}$ = 6.8 Hz, 3H, CH(CH$_3$)$_2$), 1.35 (dd, $^3J_{HH}$ = 6.8 Hz, 6H, CH(CH$_3$)$_2$), 1.32 (d, $^3J_{HH}$ = 6.7 Hz, 3H, CH(CH$_3$)$_2$), 1.28 (d, $^3J_{HH}$ = 6.6 Hz, 3H, CH(CH$_3$)$_2$), 1.27 (d, $^3J_{HH}$ = 6.8 Hz, 3H, CH(CH$_3$)$_2$), 1.24 (d, $^3J_{HH}$ = 6.7 Hz, 3H, CH(CH$_3$)$_2$), 1.18 (dd, $^3J_{HH}$ = 6.7, 2.5 Hz, 6H, CH(CH$_3$)$_2$), 1.11 (dd, $^3J_{HH}$ = 6.7 Hz, 6H, CH(CH$_3$)$_2$), 1.08 (d, $^3J_{HH}$ = 6.7 Hz, 3H, CH(CH$_3$)$_2$), −0.24 (s, 9H, CHSi(CH$_3$)$_3$). ^{13}C NMR (151 MHz, C_6D_6): δ 168.5, 168.2, 168.1, 168.1 (ArNCCH$_3$), 145.3, 145.3, 145.2, 144.8, 143.9, 143.8, 143.7, 143.5, 143.3, 142.8, 142.4, 142.1, 127.7, 127.1, 127.1, 127.1, 125.5, 125.1, 125.0, 124.8, 124.7, 124.4, 124.4, 124.3 (ArC), 97.4, 97.3 (γ-CH), 47.6, 46.7, 44.8, 44.1 (N(CH$_3$)$_2$), 30.2, 29.8, 29.3, 28.7, 28.0, 28.0, 27.9, 27.9 (CH(CH$_3$)$_2$), 27.5, 26.7, 26.5, 25.8, 25.8, 25.6, 25.5, 25.4, 25.0, 25.0, 24.9, 24.9, 24.9, 24.8, 24.7, 24.6 (CH(CH$_3$)$_2$), 24.4, 23.9, 23.7, 23.7 (ArNCCH$_3$), 3.6 (CHSi(CH$_3$)$_3$), -5.4 (CHSi(CH$_3$)$_3$). ^{29}Si NMR (79.5 MHz, C_6D_6, 25 °C): δ 2.8 (CHSi(CH$_3$)$_3$).

[L(EtO)GaSb]$_2$C(H)SiMe$_3$ (12). (L(EtO)GaSb)$_2$ (50 mg, 38 μmol) was suspended in 1 ml of toluene and 63.7 μl of a Me$_3$Si(H)CN$_2$ solution (0.6 M in *n*-hexane) was added. The resulting suspension was stirred for 12 h at room temperature. Pure **12** was obtained after removal of all volatiles *in vacuo* and washing of the slightly yellow residue with minimal amounts of cold *n*-hexane. Yield: 45 mg (32 μmol, 84%). Anal. calcd for $C_{66}H_{102}Ga_2N_4O_2Sb_2Si$: C, 54.14; H, 6.74; N, 4.07%. Found: C, 54.3; H, 6.88; N, 3.94%. ATR-IR: ν 2948, 2912, 2855, 1544, 1517, 1456, 1431, 1378, 1355, 1311, 1254, 1095, 1056, 1016, 931, 854, 791, 754, 600 cm^{-1}. ^1H NMR (400 MHz, C_6D_6, 25 °C): δ 7.3–7.17 (m, 8H, C_6H_3-2,6^{i}Pr$_2$), 7.15–7.06 (m, 4H, C_6H_3-2,6^{i}Pr$_2$), 4.75 (s, 1H, γ-CH), 4.70 (s, 1H, γ-CH), 3.93 (m, 2H, OCH$_2$CH$_3$), 3.78 (q, $^3J_{HH}$ = 6.8 Hz, 2H,

 © 2022 The Author(s). Published by the Royal Society of Chemistry

Open Access Article. Published on 03 March 2022. Downloaded on 10/28/2025 3:34:55 PM. This article is licensed under a Creative Commons Attribution-NonCommercial 3.0 Unported Licence.

OCH_2CH_3), 3.51 (m, 5H, $CH(CH_3)_2$), 3.28 (m, $CH(CH_3)_2$), 3.23 (hept, $^3J_{HH}$ = 6.7 Hz, 1H, $CH(CH_3)_2$), 2.13 (s, 1H, $CHSi(CH_3)_3$), 1.58 (d, $^3J_{HH}$ = 6.7 Hz, 3H, $CH(CH_3)_2$), 1.57 (s, 6H, $ArNCCH_3$), 1.56 (s, 6H, $ArNCCH_3$), 1.49 (s, 6H, $ArNCCH_3$), 1.49 (d, $^3J_{HH}$ = 6.9 Hz, 3H, $CH(CH_3)_2$), 1.46 (d, $^3J_{HH}$ = 6.9 Hz, 3H, $CH(CH_3)_2$), 1.45 (d, $^3J_{HH}$ = 6.9 Hz, 3H, $CH(CH_3)_2$), 1.44 (s, 6H, $ArNCCH_3$), 1.40 (d, $^3J_{HH}$ = 6.7 Hz, 3H, $CH(CH_3)_2$), 1.37 (d, $^3J_{HH}$ = 6.7 Hz, 3H, $CH(CH_3)_2$), 1.36 (d, $^3J_{HH}$ = 6.7 Hz, 3H, $CH(CH_3)_2$), 1.31 (d, $^3J_{HH}$ = 6.7 Hz, 3H, $CH(CH_3)_2$), 1.29 (d, $^3J_{HH}$ = 6.7 Hz, 3H, $CH(CH_3)_2$, 1.28–1.20 (m, 9H, $CH(CH_3)_2$ and 6H, OCH_2CH_3), 1.19 (d, $^3J_{HH}$ = 6.7 Hz, 3H, $CH(CH_3)_2$), 1.13 (d, $^3J_{HH}$ = 6.8 Hz, 3H, $CH(CH_3)_2$), 1.11 (d, $^3J_{HH}$ = 6.8 Hz, 3H, $CH(CH_3)_2$), 1.06 (d, $^3J_{HH}$ = 6.8 Hz, 3H, $CH(CH_3)_2$), 0.01 (s, 9H, $CHSi(CH_3)_3$). ^{13}C NMR (101 MHz, C_6D_6) δ 168.7, 168.6, 168.6, 168.1 ($ArNCCH_3$), 145.3, 145.3, 144.9, 144.8, 143.2, 142.9, 142.9, 142.7, 142.7, 142.7, 142.4, 142.4, 127.5, 127.5, 127.5, 127.3, 125.3, 125.2, 125.1, 124.5, 124.5, 124.4, 124.3, 124.3 (ArC), 97.6, 97.5 (γ-CH), 61.7, 61.4 (OCH_2CH_3), 30.2, 29.5, 29.4, 29.1, 27.8, 27.8, 27.8, 27.6 ($CH(CH_3)_2$), 27.1, 26.6, 26.0, 25.8, 25.6, 25.5, 25.4, 25.4, 25.0, 24.9, 24.8, 24.7, 24.6, 24.6 ($CH(CH_3)_2$), 24.3, 23.9, 23.7, 23.7, ($ArNCCH_3$), 20.7, 20.4 (OCH_2CH_3), 3.0 ($CHSi(CH_3)_3$), -3.7 ($CHSi(CH_3)_3$). ^{29}Si NMR (79.5 MHz, C_6D_6, 25 °C): δ 4.3 ($CHSi(CH_3)_3$).

$[L(Cl)GaSb]_2C(H)SiMe_3$ (13). $[L(Cl)GaSb]_2$ (80 mg, 62 μmol) was suspended in 2 ml of toluene and 103.8 μl of a $Me_3Si(H)CN_2$ solution (0.6 M in *n*-hexane) was added. The resulting suspension was stirred for 1 h at room temperature. After removing all volatiles *in vacuo*, the residue was suspended in 3 ml of *n*-hexane and stored at 4 °C for 12 h, yielding **13** as slightly orange powder. Yield: 50 mg (36 μmol, 58%). Anal. calcd for $C_{62}H_{92}Cl_2Ga_2N_4Sb_2Si$: C, 54.14; H, 6.74 N, 4.07. Found: C, 54.3; H, 6.88 N, 3.94%. ATR-IR: ν 3050, 2955, 2913, 2860, 1520, 1457, 1431, 1378, 1357, 1310, 1255, 1172, 1013, 934, 856, 830, 793, 771, 754, 637, 529 cm^{-1}. ^1H NMR (600 MHz, C_6D_6, 25 °C): δ 7.28–7.21 (m, 4H, C_6H_3-2,6^{i}Pr$_2$), 7.15–7.03 (m, 8H, C_6H_3-2,6^{i}Pr$_2$), 4.92 (s, 1H, γ-CH), 4.81 (s, 1H, γ-CH), 3.72 (sept, $^3J_{HH}$ = 6.7 Hz, 1H, $CH(CH_3)_2$), 3.58 (sept, $^3J_{HH}$ = 6.8 Hz, 1H, $CH(CH_3)_2$), 3.54 (sept, $^3J_{HH}$ = 6.6 Hz, 1H, $CH(CH_3)_2$), 3.53 (sept, $^3J_{HH}$ = 6.8 Hz, 1H, $CH(CH_3)_2$), 3.48 (sept, $^3J_{HH}$ = 6.7 Hz, 1H, $CH(CH_3)_2$), 3.41 (sept, $^3J_{HH}$ = 6.8 Hz, 1H, $CH(CH_3)_2$), 3.29 (sept, $^3J_{HH}$ = 6.8 Hz, 1H, $CH(CH_3)_2$), 3.25 (sept, $^3J_{HH}$ = 6.8 Hz, 1H, $CH(CH_3)_2$), 2.18 (s, 1H, $CHSi(CH_3)_3$), 1.56 (s, 6H, $ArNCCH_3$), 1.53 (d, $^3J_{HH}$ = 7.1 Hz, 3H, $CH(CH_3)_2$), 1.53 (s, 6H, $ArNCCH_3$), 1.50 (d, $^3J_{HH}$ = 7.0 Hz, 3H, $CH(CH_3)_2$), 1.48 (d, $^3J_{HH}$ = 6.9 Hz, 3H, $CH(CH_3)_2$), 1.46 (s, 6H, $ArNCCH_3$), 1.45 (d, $^3J_{HH}$ = 7.0 Hz, 3H, $CH(CH_3)_2$), 1.40 (s, 6H, $ArNCCH_3$), 1.38 (d, $^3J_{HH}$ = 6.9 Hz, 3H, $CH(CH_3)_2$), 1.35 (d, $^3J_{HH}$ = 6.7 Hz, 3H, $CH(CH_3)_2$), 1.32 (d, $^3J_{HH}$ = 6.6 Hz, 3H, $CH(CH_3)_2$), 1.27 (d, $^3J_{HH}$ = 6.8 Hz, 3H, $CH(CH_3)_2$), 1.25 (d, $^3J_{HH}$ = 68 Hz, 3H, $CH(CH_3)_2$), 1.22 (d, $^3J_{HH}$ = 6.8 Hz, 3H, $CH(CH_3)_2$), 1.13 (d, $^3J_{HH}$ = 6.7 Hz, 6H, $CH(CH_3)_2$), 1.09 (d, $^3J_{HH}$ = 6.9 Hz, 3H, $CH(CH_3)_2$), 1.09 (d, $^3J_{HH}$ = 6.7 Hz, 3H, $CH(CH_3)_2$), 1.04 (d, $^3J_{HH}$ = 6.7 Hz, 3H, $CH(CH_3)_2$), 1.00 (d, $^3J_{HH}$ = 6.7 Hz, 3H, $CH(CH_3)_2$), −0.13 (s, 9H, $CHSi(CH_3)_3$). ^{13}C NMR (151 MHz, C_6D_6): δ 169.1, 168.6, 168.5, 168.3 ($ArNCCH_3$), 145.9, 145.9, 145.6, 145.6, 142.8, 142.4, 142.3, 142.1, 142.1, 141.9, 141.7, 141.3, 128.1, 128.0, 126.1, 126.0, 125.6, 125.2, 124.4, 124.2, 124.1, 124.1 (ArC), 98.1, 97.9 (γ-CH), 30.6, 30.4, 29.7, 29.7, 28.2, 28.0, 28.0, 27.8 ($CH(CH_3)_2$), 28.4, 27.6, 27.1, 26.7, 25.5, 25.1, 25.1, 25.1, 25.0, 24.9, 24.8, 24.6, 24.5, 24.3, 24.2, 24.2 ($CH(CH_3)_2$), 24.3, 24.0, 23.9, 23.8 ($ArNCCH_3$), 3.5 ($CHSi(CH_3)_3$), 1.6 ($CHSi(CH_3)_3$). ^{29}Si NMR (119.2 MHz, C_6D_6, 25 °C): δ 3.8 ($CHSi(CH_3)_3$).

Data availability

Spectroscopic (NMR, IR, UV-Vis) and crystallographic data (cif file) are provided.

Author contributions

M. W. performed the experiments including quantum chemical calculations, C. W. the single crystal X-ray diffraction. The work was supervised by S. S. The manuscript was written through contributions of all authors. All authors have given approval to the final version of the manuscript.

Conflicts of interest

There are no conflicts to declare.

Acknowledgements

We are thankful to the Deutsche Forschungsgemeinschaft DFG (St.S., SCHU 1069/22-3) for generous financial support.

Notes and references

1 (*a*) C. Weetman, *Chem.–Eur. J.*, 2021, **27**, 1941; (*b*) C. Weetman and S. Inoue, *ChemCatChem*, 2018, **10**, 4213; (*c*) T. Chu and G. I. Nikonov, *Chem. Rev.*, 2018, **118**, 3608; (*d*) P. P. Power, *Chem. Rec.*, 2012, **12**, 238; (*e*) P. P. Power, *Nature*, 2010, **463**, 171.

2 (*a*) M. Breugst and H.-U. Reissig, *Angew. Chem., Int. Ed. Engl.*, 2020, **59**, 12293; (*b*) O. Diels and K. Alder, *Justus Liebigs Ann. Chem.*, 1928, **460**, 98; (*c*) R. Huisgen, *Angew. Chem., Int. Ed. Engl.*, 1963, **2**, 633; (*d*) R. Huisgen, *Angew. Chem.*, 1963, **75**, 604.

3 F. Hanusch, L. Groll and S. Inoue, *Chem. Sci.*, 2021, **12**, 2001.

4 (*a*) L. Weber, *Chem. Rev.*, 1992, **92**, 1839; (*b*) M. Yoshifuji, *Pure Appl. Chem.*, 2017, **89**, 281; (*c*) D. Nauroozi and A. Orthaber, *Eur. J. Inorg. Chem.*, 2016, **2016**, 709; (*d*) R. K. Bansal and S. K. Kumawat, *Tetrahedron*, 2008, **64**, 10945; (*e*) J. D. Protasiewicz, in *Comprehensive inorganic chemistry II. From elements to applications*, ed. J. Reedijk, Elsevier, Amsterdam, 2nd edn, 2013, pp. 325–348; (*f*) M. Yoshifuji, *Eur. J. Inorg. Chem.*, 2016, 607.

5 (*a*) H.-J. Himmel, *Eur. J. Inorg. Chem.*, 2153, **2003**, 2003; (*b*) H. Voelker, U. Pieper, H. W. Roesky and G. M. Sheldrick, *Z. Naturforsch., B: J. Chem. Sci.*, 1994, **49**, 255; (*c*) T. Sasamori, E. Mieda, N. Takeda and N. Tokitoh, *Chem. Lett.*, 2005, **33**, 104; (*d*) T. Sasamori, E. Mieda, N. Takeda and N. Tokitoh, *Angew. Chem., Int. Ed.*, 2005, **44**, 3717; *Angew. Chem.*, 2005, **117**, 3783; (*e*) T. Sasamori, E. Mieda and N. Tokitoh, *Bull. Chem. Soc. Jpn.*, 2007, **80**, 2425; (*f*) T. Sasamori, N. Takeda and N. Tokitoh, *J. Phys. Org. Chem.*, 2003, **16**, 450; (*g*) M. Ateş, H. J. Breunig, S. Güleç, W. Offermann, K. Häberle and M. Dräger, *Chem. Ber.*, 1989, **122**, 473; (*h*) L. Dostál,

Open Access Article. Published on 03 March 2022. Downloaded on 10/28/2025 3:34:55 PM.
This article is licensed under a Creative Commons Attribution-NonCommercial 3.0 Unported Licence.

R. Jambor, A. Růžička and J. Holeček, *Organometallics*, 2008, **27**, 2169; (*i*) S. S. Chitnis, A. P. M. Robertson, N. Burford, J. J. Weigand and R. Fischer, *Chem. Sci.*, 2015, **6**, 2559; (*j*) S. S. Chitnis, Y.-Y. Carpenter, N. Burford, R. McDonald and M. J. Ferguson, *Angew. Chem., Int. Ed.*, 2013, **52**, 4863; (*k*) S. S. Chitnis, Y.-Y. Carpenter, N. Burford, R. McDonald and M. J. Ferguson, *Angew. Chem.*, 2013, **125**, 4963.

6 (*a*) J. Grobe, A. Karst, B. Krebs, M. Läge and E.-U. Würthwein, *Z. Anorg. Allg. Chem.*, 2006, **632**, 599; (*b*) I. Jibril, L.-R. Frank, L. Zsolnai, K. Evertz and G. Huttner, *J. Organomet. Chem.*, 1990, **393**, 213; (*c*) G. Huttner and I. Jibril, *Angew. Chem.*, 1984, **96**, 709; (*d*) T. Umeyama, K. Naka and Y. Chujo, *J. Polym. Sci., Part A: Polym. Chem.*, 2004, **42**, 3023; (*e*) A. Karst, B. Broschk, J. J. Grobe and D. Le Van, *Z. Naturforsch., B: J. Chem. Sci.*, 1995, **50**, 189.

7 (*a*) N. Tokitoh, Y. Arai, T. Sasamori, R. Okazaki, S. Nagase, H. Uekusa and Y. Ohashi, *J. Am. Chem. Soc.*, 1998, **120**, 433; (*b*) T. Sasamori, E. Mieda, N. Nagahora and N. Tokitoh, *Chem. Heterocycl. Compd.*, 2006, **42**, 1603.

8 (*a*) T. Sasamori, E. Mieda, N. Takeda and N. Tokitoh, *Chem. Lett.*, 2004, **33**, 104; (*b*) T. Sasamori, E. Mieda, A. Tsurusaki, N. Nagahora and N. Tokitoh, *Phosphorus, Sulfur Silicon Relat. Elem.*, 2008, **183**, 998; (*c*) N. Tokitoh, T. Sasamori and R. Okazaki, *Chem. Lett.*, 1998, **27**, 725; (*d*) T. Sasamori and N. Tokitoh, *Dalton Trans.*, 2008, 1395.

9 (*a*) L. Tuscher, C. Ganesamoorthy, D. Bläser, C. Wölper and S. Schulz, *Angew. Chem., Int. Ed.*, 2015, **54**, 10657; *Angew. Chem.*, 2015, **127**, 10803; (*b*) L. Tuscher, C. Helling, C. Ganesamoorthy, J. Krüger, C. Wölper, W. Frank, A. S. Nizovtsev and S. Schulz, *Chem.–Eur. J.*, 2017, **23**, 12297; (*c*) L. Tuscher, C. Helling, C. Wölper, W. Frank, A. S. Nizovtsev and S. Schulz, *Chem.–Eur. J.*, 2018, **24**, 3241; (*d*) J. Krüger, J. Schoening, C. Ganesamoorthy, L. John, C. Wölper and S. Schulz, *Z. Anorg. Allg. Chem.*, 2018, **644**, 1028; (*e*) L. Song, J. Schoening, C. Wölper, S. Schulz and P. R. Schreiner, *Organometallics*, 2019, **38**, 1640.

10 (*a*) H. M. Weinert, C. Wölper, J. Haak, G. E. Cutsail III and S. Schulz, *Chem. Sci.*, 2021, **12**, 14024; (*b*) H. M. Weinert, C. Wölper and S. Schulz, *Organometallics*, 2021, **40**, 3486.

11 (*a*) E. Niecke, R. Rüger, M. Lysek and W. W. Schoeller, *Phosphorus Sulfur Relat. Elem.*, 1983, **18**, 35; (*b*) J. Borm, G. Huttner and O. Orama, *J. Organomet. Chem.*, 1986, **306**, 29; (*c*) J. Borm, G. Huttner, O. Orama and L. Zsolnai, *J. Organomet. Chem.*, 1985, **282**, 53; (*d*) W. Güth, PhD thesis, University of Bielefeld, 1987, pp. 12–15.

12 K. Schwedtmann, F. Hennersdorf, A. Bauzá, A. Frontera, R. Fischer and J. J. Weigand, *Angew. Chem., Int. Ed.*, 2017, **56**, 6218.

13 J. A. B. Abdalla, I. M. Riddlestone, R. Tirfoin and S. Aldridge, *Angew. Chem., Int. Ed.*, 2015, **54**, 5098.

14 C. Klmel, C. Ochsenfeld and R. Ahlrichs, *Theor. Chim. Acta*, 1992, **82**, 271.

15 P. Vilarrubias, *Mol. Phys.*, 2017, **115**, 2597.

16 (*a*) R. J. Schwamm and M. P. Coles, *Chem.–Eur. J.*, 2019, **25**, 14183; (*b*) D. Dange, A. Davey, J. A. B. Abdalla, S. Aldridge and C. Jones, *Chem. Commun.*, 2015, **51**, 7128.

17 M. Miar, A. Shiroudi, K. Pourshamsian, A. R. Oliaey and F. Hatamjafari, *J. Chem. Res.*, 2021, **45**, 147.

18 Cambridge Structural Database, Version 5.42, see also: F. H. Allen, *Acta Crystallogr. Sect. B*, 2002, **58**, 380–388. 55 hits containing an Sb–Sb bond classified as a single were found of the type $R_2Sb–SbR_2$ (R defined as non-antimony, c.n. (Sb) = 3). The Sb–Sb bond lengths range from 2.77–3.07 Å (mean of 2.86(5) Å excluding a single highly ring strain structure 2.64 Å.

19 Cambridge Structural Database, Version 5.42, see also: F. H. Allen, *Acta Crystallogr. Sect. B*, 2002, **58**, 380–388. 495 hits containing an Sb–C bond classified as a single were found of the type $R_2Sb–C$ (c.n. (Sb) = 3). The Sb-C bond lengths range from 2.04–2.31 Å (mean of 2.17(4)). Analogous, 195 entries for Sb–N were found, 1.95–2.58 Å (mean of 2.06(7)).

20 The ORCA quantum chemistry package was used and details regarding the quantum chemical calculations are given in the ESI.† (*a*) F. Neese, *Wiley Interdiscip. Rev.: Comput. Mol. Sci.*, 2012, **2**, 73; (*b*) F. Neese, F. Wennmohs, U. Becker and C. Riplinger, *J. Chem. Phys.*, 2020, **152**, 224108; (*c*) F. Neese, *Wiley Interdiscip. Rev. Comput. Mol. Sci.*, 2018, **8**, 1; (*d*) C. Adamo and V. Barone, *J. Chem. Phys.*, 1999, **110**, 6158; (*e*) F. Weigend and R. Ahlrichs, *Phys. Chem. Chem. Phys.*, 2005, **7**, 3297; (*f*) S. Grimme, J. Antony, S. Ehrlich and H. Krieg, *J. Chem. Phys.*, 2010, **132**, 154104; (*g*) S. Grimme, S. Ehrlich and L. Goerigk, *J. Comput. Chem.*, 2011, **32**, 1456; (*h*) B. Metz, H. Stoll and M. Dolg, *J. Chem. Phys.*, 2000, **113**, 2563; (*i*) R. Izsák and F. Neese, *J. Chem. Phys.*, 2011, **135**, 144105; (*j*) F. Neese, F. Wennmohs, A. Hansen and U. Becker, *Chem. Phys.*, 2009, **356**, 98; (*k*) F. Weigend, *Phys. Chem. Chem. Phys.*, 2006, **8**, 1057; (*l*) M. Garcia-Ratés and F. Neese, *J. Comput. Chem.*, 2020, **41**, 922; (*m*) M. Cossi, N. Rega, G. Scalmani and V. Barone, *J. Comput. Chem.*, 2003, **24**, 669; (*n*) V. Barone and M. Cossi, *J. Phys. Chem. A*, 1998, **102**, 1995

21 (*a*) P. Jutzi and S. Opiela, *Z. Anorg. Allg. Chem.*, 1992, **610**, 75; (*b*) G. Etemad-Moghadam, J. Bellan, C. Tachon and M. Koenig, *Tetrahedron*, 1987, **43**, 1793.

22 NBO 7.0, E. D. Glendening, J. K. Badenhoop, A. E. Reed, J. E. Carpenter, J. A. Bohmann, C. M. Morales, P. Karafiloglou, C. R. Landis, and F. Weinhold, *Theoretical Chemistry Institute*, University of Wisconsin, Madison, WI, 2018.

23 W. Humphrey, A. Dalke and K. Schulten, *J. Mol. Graphics*, 1996, **14**, 33–38, http://www.ks.uiuc.edu/Research/vmd/.

24 (*a*) R. D. Bach and O. Dmitrenko, *J. Am. Chem. Soc.*, 2004, **126**, 4444; (*b*) K. B. Wiberg and R. A. Fenoglio, *J. Am. Chem. Soc.*, 1968, **90**, 3395.

25 (*a*) P. S. V. Kumar, V. Raghavendra and V. Subramanian, *J. Chem. Sci.*, 2016, **128**, 1527; (*b*) R. F. W. Bader, *Chem. Rev.*, 1991, **91**, 893; (*c*) C. Kalaiarasi, M. S. Pavan and P. Kumaradhas, *Acta Crystallogr., Sect. B: Struct. Sci., Cryst. Eng. Mater.*, 2016, **72**, 775; (*d*) T. Lu and F. Chen, *J. Comput. Chem.*, 2012, **33**, 580.

26 (*a*) U. Ekström, L. Visscher, R. Bast, A. J. Thorvaldsen and K. Ruud, *J. Chem. Theory Comput.*, 2010, **6**, 1971; (*b*) B. Silvi and A. Savin, *Nature*, 1994, **371**, 683; (*c*) A. D. Becke and K. E. Edgecombe, *J. Chem. Phys.*, 1990, **92**, 5397.

 © 2022 The Author(s). Published by the Royal Society of Chemistry